University of Alberta

Detection of Shiga Toxin-Producing *Escherichia coli* Using Loop Mediated Isothermal Amplification

by

Richelle Allen

A thesis submitted to the Faculty of Graduate Studies and Research
in partial fulfillment of the requirements for the degree of

Master of Science

Medical Sciences - Laboratory Medicine and Pathology

Fall 2013
Edmonton, Alberta

Dedication:

I dedicate this thesis to my father, Tim Allen. You were the hardest working; most amazing person I know and you were taken too soon. You inspired me to always push harder and take that next step, even when it wasn't easy. I took a path in life you may not have understood but you always supported me 100% and for that I will be forever grateful.

Abstract:

Shiga toxin-producing Escherichia coli (STEC) is a worldwide health concern. To detect STEC, a loop mediated isothermal amplification reaction (LAMP) was optimized to detect shiga toxin genes. LAMP's performance was compared to conventional and real-time (RT) PCR using two product detection methods. All three DNA amplification methods produced similar results. LAMP performed well when tested with randomly selected stool samples. LAMP, with agarose gel detection, showed a sensitivity of 90%/100%, specificity of 95%/99%, a positive predictive value of 56%/89% and a negative predictive value of 99%/100% for stx1 and stx2 respectively. Sybr Green 1 detection had a sensitivity of 100%/100%, specificity of 93%/77%, positive predictive values of 76/39% and negative predictive values of 100/100% for stx1 and stx2 respectively. Per 10 tests LAMP costs approximately $45, when using a rapid lysis DNA extraction and agarose gel electrophoresis product detection. LAMP could be implemented in laboratories without dedicated molecular biology facilities.

Acknowledgements:

I wish to express my gratitude to the following individuals, without whom my thesis could not have been completed:

Dr. Linda Chui, my supervisor throughout my graduate program.

Dr. Monika Keelan, for all of your help and encouragement throughout my degree.

The BTU team (Linda, Patricia, Theo, Vince, Martha, Donna and Sylvia) at the Provincial Laboratory for your friendship, encouragement and willingness to lend a hand whenever it was needed.

My friends and family, who have put up with my long hours and neglect during my degree yet have always been there for me when I needed them.

To Bob Sargent, John Rew and Darlene Herzog, knowing you guys were taking care of things back home is the reason I was able to come back and finish my degree. I will be forever grateful to all you have done for my family.

To Andrew Redekop, your understanding, support and willingness to help in any way possible throughout this thesis has been amazing.

To my parents, Tim and Joanne Allen, who have always been there for me and encouraged me no matter what. Your drive to succeed and work ethic has always been my inspiration.

Table of Contents

List of Tables:

List of Figures:

List of Symbols, Nomenclature or Abbreviations:

A/E	Attachment and Effacing
AOLR	Areas of limited resources
ASSURED	Affordable, Sensitive, Specific, User-friendly, Rapid and robust, Equipment free and Deliverable.
B3	Backward outer primer
BAP	Blood agar plate
BIP	Backward inner primer
CDC	Center for Disease Control and Prevention
DAEC	Diffusely Adherent *Escherichia coli*
EAHEC	Enteroaggregative Hemorrhagic *Escherichia coli*
EHEC	Enterohemorrhagic *Escherichia coli*
EIEC	Enteroinvasive *Escherichia coli*
EPEC	Enteropathogenic *Escherichia coli*
ETEC	Enterotoxigenic *Escherichia coli*

EIA	Enzyme Immunoassay
ER	Endoplasmic Reticulum
F3	Forward outer primer
FIP	Forward inner primer
Gb3	Globotriaosylceramide 3
GB4	Globotetraosylceramide 4
H	Flagellar Antigen
HC	Hemorrhagic colitis
HUS	Hemolytic Uremic Syndrome
K	Capsular Antigen
LAMP	Loop Mediated Isothermal Amplification
LB	Loop backward primer
LEE	Locus of Enterocycte Effacement
LF	Loop forward primer
MAHA	Microangiopathic Hemolytic Anemia
:NM	Non-motile

O	Heat stable somatic antigen
PCR	Polymerase Chain Reaction
RT-PCR	Real time PCR
STEC	Shiga-Toxin Producing *Escherichia coli*
Stx_1	Shiga toxin 1 gene
Stx_2	Shiga toxin 2 gene
Stx	Shiga toxin protein
TIR	Translocated Intimin Receptor
T3SS	Type 3 Secretion System
UPEC	Uropathogenic *Escherichia coli*
ProvLab	Provincial Laboratory for Public Health
TAT	Turn-around-time
SG1	Sybr Green I
UV	Ultraviolet

Chapter 1: Introduction

1.1 Overview

Escherichia coli is a Gram negative facultative anaerobic bacterium that is a component of the normal flora of the human gastrointestinal tract (1, 2). In most cases, *E. coli* is non-pathogenic in humans and is even beneficial to the human host, as it helps to suppress colonization of pathogenic bacteria that are harmful to the host (1-3). However, not all strains of *E. coli* are harmless, certain strains have developed the ability to cause diseases ranging from urinary tract infections, to diarrheal disease, to sepsis (2, 3). The main classifications of pathogenic *E. coli* are enteropathogenic (EPEC), shiga-toxin producing (STEC), enteroaggregative (EAEC), enterotoxigenic (ETEC), enteroinvasive (EIEC), diffusely adherent (DAEC) and uropathogenic (UPEC). This thesis will focus on the shiga toxin-producing category of pathogenic *E. coli* (1-3).

Shiga-toxin producing *E. coli* (STEC) are pathogens of the human gastrointestinal tract that cause severe abdominal cramps and in some cases bloody diarrhea (1). In more severe cases symptoms may progress to potentially life-threatening complications such as hemorrhagic colitis (HC) and hemolytic uremic syndrome (HUS). Both conditions result from shiga toxin induced tissue damage, to intestinal tissue in the case of hemorrhagic colitis and the vascular endothelium of the kidney in the case of hemolytic uremic syndrome (4). The natural reservoirs of STEC are ruminants, such as cattle and sheep (1, 3, 5). Humans become infected with STEC when they come into contact with colonized animals, or following consumption of contaminated water, raw milk or food products, such as undercooked meat (4). The first documented outbreak of STEC, specifically *E. coli* O157:H7, occurred in the United States in 1982 and it has been an important pathogen ever since (6). Recent estimates by the Centers for Disease Control and Prevention (CDC) in Atlanta, USA, have indicated that at least 73 000 cases of STEC O157 infections occur each year in the United States, with 1493 of these requiring hospitalizations and 40 resulting in deaths (6).

Currently, STEC is diagnosed using culture-based techniques, such as plating stool samples onto Sorbital MacConkey agar (SMAC) or ChromAgar O157, as well as by confirmation with serological techniques to detect bacterial surface antigens such as O157 (7). However, although these culture-based and serological methods are effective for *E. coli* O157:H7, non-O157 STEC are under diagnosed. Non-O157 STEC tend to be missed as current culture-based methods do not detect the shiga toxin itself, and instead rely on detecting the inability of O157:H7 to ferment sorbitol. As non-O157 STEC strains are able to ferment sorbitol they will be missed by culture-based methods. In addition, these methods are practical only for well-funded and well-equipped microbiology dedicated diagnostic laboratories and are impractical for developing nations/areas of limited resources due to the cost (incubators, media), expertise required, and difficulty of obtaining the equipment needed for such assays (8). In 2009, in response to increasing outbreaks caused by non-O157 STEC, the Centre for Disease Control and Prevention (CDC) recommended new guidelines to test for all STEC by EIA (enzyme immunoassay), to detect shiga toxin protein, or nucleic acid testing, to detect the shiga toxin genes (7). PCR (polymerase chain reaction) and EIA methods for detecting STEC have been developed; however, they are expensive, may be subject to inhibition from biological samples (PCR), and require well-trained staff (7)

1.2 Escherichia coli

Escherichia coli, originally known as *Bacterium coli commune,* was first discovered in 1885 by the pediatrician Theodor Escherich (9). Most strains of *E. coli* are harmless, and are commensals of the human gastrointestinal tract (10). These non-pathogenic varieties of *E. coli* may acquire genetic elements such as plasmid DNA or bacteriophages that encode virulence genes, such as *stx*, making them harmful to humans (10).

The ability to serogroup *E. coli* as a means of differentiating between different types or ‘serogroups’ was first discovered in 1943 by Fritz Kauffman who found that different serogroups of the bacteria had distinctive surface antigens (10). This system of serogrouping, which is still used today, detects the

O (heat stable somatic antigen), H (flagellar antigen) and sometimes K (capsular antigen) of the bacteria (10). The serogroup is then named based upon the particular combination of surface antigens it possesses, for example *E. coli* O157:H7 or O104:H4 (10). Currently, over 170 O antigens and over 56 H antigens have been discovered (10).

Originally, the only shiga toxin producing form of *E. coli* was thought to be O157:H7 and as such it has become the most well known form of STEC. Other serotypes of *E. coli,* such as O26, O111, and O103, were later found to be able to produce shiga toxins and these were simply known as non-O157 STEC (7). Both O157 and non-O157 serotypes that produce shiga toxins are collectively known as STEC (7).

1.3 Shiga Toxin Producing *Escherichia coli* (STEC) Infections

1.3.1 The First Recorded and Subsequent Outbreaks of STEC O157:H7

In 1982 the world's first recorded outbreak of STEC O157:H7 occurred in the United States, specifically Michigan and Oregon (11). At this time O157:H7 was a relatively unknown pathogen and it was some time before the reported symptoms of bloody diarrhea, and severe abdominal pain, with or without low-grade fever were associated with O157 (6, 11).

After the US outbreak of 1982 STEC O157:H7 outbreaks were more frequently identified due in part to increased awareness of the pathogen. Since the mid-1990's, over 180 STEC O157:H7 associated outbreaks have occurred in the United States alone (12). The increased incidence of infection led to STEC O157:H7 becoming a nationally notifiable infection in 1994 with reporting of the infection mandatory in 48 states by 2000 (6). Between 1982 and 2000 most outbreaks were associated with food, primarily ground beef (6). Sprouts, lettuce, spinach, water, raw milk cheese, ready-to-eat cookie dough, and unshelled hazelnuts have also been implicated in O157:H7 outbreaks (12-14). The first case associated with animal contact was documented in 1996 (6). Associations between STEC O157:H7 infection and food led to improvements in food safety including a new set of guidelines involving the temperature of cooking ground

beef (6). Similarly, the link between O157:H7 and livestock led to the implementation of laws which regulated animal handling at exhibitions, fairs and other venues where animals and humans have direct contact (15). One such law, Aedin's Law, was developed after O157:H7 was associated with multiple outbreaks during state fairs in North Carolina between 2004 and 2011 (15).

One of the most well known O157:H7 outbreaks occurred in Walkerton, Ontario, a small Canadian farming community in May 2000 (16, 17). The Walkerton outbreak is considered one of the largest outbreaks of O157:H7 in the world and Canada's worst public health disaster involving a municipal water supply (17). During the course of the outbreak, 2300 people in the community of 5000 became ill, 564 of which were children. Of those affected, 24 individuals developed hemolytic uremic syndrome (HUS) due to STEC infection and 7 died (16, 17). This outbreak, which has become known as the 'Walkerton Tragedy', highlights the implications of O157:H7 infection and the importance of vigilant water supply monitoring (17).

1.3.2 Outbreaks of non-O157 STEC

Although focus has historically been on O157:H7 STEC infections, recent outbreaks of non-O157 STEC have revealed non-O157 STEC to be an equally important human pathogen (18-22). The lack of awareness of non-O157 STEC has likely stemmed from an absence of screening in most laboratories. This is supported by estimates that between 2000 and 2006, the rate of non-O157 STEC detection increased by 3 fold, likely due to the implementation of shiga toxin gene testing by some labs rather than exclusive reliance on selective media that only detect STEC O157 (22).

The 2011 European outbreak of O104:H4 has served to emphasize the importance of non-O157 STEC as a human pathogen (23). Over the course of this outbreak, attributed to contaminated fenugreek seeds, over 4075 illnesses were reported in 16 countries (23). Approximately 22% of all individuals infected developed HUS and 50 deaths were reported (23). In contrast to O157 STEC infection, a large proportion of adults were infected, specifically adult women

(20). The unprecedented spread of the O104:H4 outbreak strain among the human population in Europe and its high virulence has challenged the previous classification of non-O157 STEC as a less important pathogen than O157 (20).

Although the O104:H4 outbreak has served as the 'posterchild' for non-O157 STEC infections, there have been many previously documented cases of non-O157 outbreaks. In June 2010, a childcare center in Colorado, USA, experienced an outbreak of O26:H11 leading to illness in approximately 45 children (18). This outbreak was likely due to multiple, repeated violations of sanitary procedures leading to person-person transmission of the pathogen amongst staff and children (18). In another case of poor hygiene practices, an outbreak of O111 STEC occurred in a Colorado corrections facility where inmates worked with dairy cattle and frequently travelled between barns and kitchen facilities (19). In 2010, a non-hygiene related STEC outbreak of O145:NM, linked to shredded romaine lettuce, occurred across 5 states resulting in 26 illnesses of which 35% required hospitalization and 10% developed HUS (21).

1.3.3 Incidence of Infection

The true incidence of STEC infection worldwide is understudied; however, some countries with surveillance programs have made annual statistics available. The Public Health Agency of Canada estimated the incidence of *E.coli* O157 infection to be 1.39 per 100 000 people in 2012; however, no data was available for non-O157 infection (24). Non-O157 STEC is estimated to cause 169 000 illnesses in the United States alone and accounts for 40-50% of all STEC infections (18, 22). Australian statistics derived from 2000 to 2010 have shown an average yearly incidence of STEC infection of 0.4 cases per 100 000 people (25).

1.3.4 Common Reservoirs of STEC

The most common reservoir of STEC is cattle; however, other ruminants, such as sheep, also harbor the organism (3, 26-28). STEC follows the 'Sink-Source' model of infection where ruminants are the 'source' of infection and humans represent the 'sink' (3). In the 'source' (ruminants), STEC are not

pathogenic, while in the ‘sink’ (humans) the organism is pathogenic and not able to survive and propagate long term, and thus represents a dead-end for the organism (3). The prevalence of O157 STEC is dynamic and it is estimated that between 0.2 and 48.8% of cattle carry STEC at any given time (3). Factors that induce stress in herds such as cattle type, movement and weaning are known to increase rates of STEC carriage (3). Although ruminants are the primary sources of infection, non-ruminants such as pigs may also carry STEC (27). Wildlife are not considered a significant source of STEC; however, the presence of STEC has been documented in amphibians, fish and insects (27). Insects, in particular flies, may be an important method of transmission as they may carry the pathogen to naïve cattle, and deposit it on food sources (27).

1.3.5 Transmission of Infection

1.3.5.1 Foodborne

In the majority of STEC outbreaks, food has been confirmed as the source of infection (3). A study of 90 outbreaks throughout continental Europe, the UK, Japan and North America between 1982 and 2006 found that in 42.2% of the 90 outbreaks the source of the organism was food (3). Contaminated ground beef tends to be the most common source; however, cheese, milk and vegetables are also often implicated as carriers in STEC infections (3, 29-35). Although ground beef is the food product most commonly associated with contamination, the two largest foodborne outbreaks that have occurred to date have been associated with sprouts. The 1996 Sakai City outbreak in Japan, which resulted in nearly 8000 illnesses, was due to contaminated white radish sprouts, while the 2011 O104:H4 outbreak in Germany was suspected to be due to fenugreek sprouts (29, 30). In many cases, it can be difficult to determine the source of a food-borne outbreak due to foods often being complex mixtures that may contain multiple food ingredients, both obtained locally and globally (14).

Meat products may become contaminated with STEC in a variety of ways and at various points during the farm to table continuum (35). Ruminants, cattle in particular, are the natural reservoirs of STEC and carry the pathogen asymptomatically while shedding the organisms in their feces (3, 36-39). STEC carriage in cattle is dynamic, with an increase of prevalence in the summer and fall, which corresponds to the time most outbreaks occur (3, 40). Cattle are more likely to shed STEC when subject to stressors in their environment such as movement (such as would occur before slaughter), weaning, and breeding (3). Those ruminants that become colonized with STEC at the lymphoid follicle dense mucosal region proximal to the recto-anal junction are more likely to shed STEC in large numbers ($>10^4$ CFU (colony forming units)/g feces) and are termed 'super-shedders' (3, 38). These super-shedders, which represent approximately 20% of the STEC infected animals, are the cause of 80% of STEC transmission (3, 38). A 2009 study by Arthur *et al.,* found that at least once during the study period 100% of study animals had O157 on their hides, 81% shed O157 in their feces, and 32% of animals shed at high levels (38). This shedding of STEC in the feces of carrier animals may lead to the colonization of naïve animals through fecal-oral transmission due to contaminated feed, water and grazing areas (28). Once cattle leave the farm for slaughter, they may be transported with cattle from other herds, increasing chances of STEC cross contamination (38).

Once at the abattoir, the hides of contaminated cattle are a major food safety concern, as during skinning, bacteria from the hides may be transferred to the carcass (12, 34, 36, 38, 40). In addition, skinned carcasses may come into contact with the contaminated carcasses with hides still intact. Interventions such as washing hides with antimicrobial agents are applied in order to reduce risk of carcass contamination; however, these are not always successful (38). There is also evidence that bacteria may penetrate the hide during the washing process and

contaminate the carcass (39). A 2007 study by Mather *et al.,* that followed 256 cattle from the farm to slaughter found 55% of the cattle's hides carried STEC (37). These STEC contaminated carcasses then have the potential to enter the food chain and cause illness.

STEC is also known to be a contaminant in produce, such as sprouts, leafy greens and vegetables, causing food-borne illness (3, 14, 29, 30, 33, 35). An increase in the number of produce-related outbreaks has correlated with the promotion of fresh fruit and vegetables as part of a healthy diet (29). The tendency to consume many of these products raw has increased the likelihood of infection, as bacteria are not likely to be removed by washing (29). As it is common to consume produce in combinations with other products, as in salads, determining the source of contamination is often difficult (29). Like meat products, produce can be contaminated at various points during the farm-fork continuum (35). Contamination may occur due to the use of untreated manure to fertilize soil, contaminated irrigation water, contact with infected animals and insects, as well as improper storage and preparation (29, 35). The numerous points at which produce may become contaminated makes determining how contamination occurred very difficult. It is still unknown how the fenugreek sprouts became contaminated in association with the 2011 O104:H4 outbreak (30).

Once produce is contaminated, it may be difficult to eliminate pathogens by common disinfection procedures. Post-harvest chemical sanitizers are routinely applied to produce (33, 35). However, evidence that pathogens may form biofilms on the plant surface, and that the pathogen may be able to contaminate the plant internally, limit the efficacy of such sanitation procedures (33, 35). Whether STEC can contaminate plants internally is still controversial; however, if true, produce sanitation methods will have to be reviewed, as surface sanitation will not be sufficient to eliminate pathogens in plant tissues (35).

Foods may also be contaminated during preparation in the home or in commercial settings. An outbreak in a Colorado correctional facility was likely due to workers wearing soiled clothes from barns in kitchens where food preparation occurred, thus allowing STEC to contaminate food (19). Poor disinfection procedures in areas where food is handled also contribute to the contamination of food by STEC (18, 19).

1.3.5.2 Water Contamination

Transmission of STEC through contaminated water sources is estimated to make up between 6-7% of all STEC infections (3). Water may be a source of infection through excessive rainfall resulting in contaminated groundwater entering the water system, improper disinfection procedures, and swimming in contaminated lakes/swimming pools (16, 17, 41-43). Studies have shown that STEC can survive up to 10 weeks in water at 25°C; therefore, proper disinfection and drainage procedures to prevent and eliminate contamination are crucial (43).

The best example of a water-associated outbreak to date is the 'Walkerton Tragedy', which occurred in Ontario in May 2000. During this outbreak, 2300 individuals in a community of 5000 became ill, 24 developed HUS and 7 died (16, 17). The initial outbreak-causing event was the heavier than normal rainfall resulting in large amounts of surface run-off entering the municipality's water supply (16, 17). The surface run-off that entered the wells was contaminated with *E.coli* O157:H7 and *Campylobacter jejuni* from the manure of a nearby farm. The contaminated wells were surrounded by farmland, poorly maintained and too shallow to protect them from groundwater contamination (16, 42).

The individuals responsible for maintenance of the wells, either through lack or training or indifference, failed to keep the wells chlorinated at levels necessary for a bactericidal effect, and often failed to monitor the wells altogether (17). When using chlorination as a method of water disinfection, it is important to note that the bactericidal effect comes from

free non-ionized chlorine (43). Free non-ionized chlorine rapidly dissipates from water and weakens with time; as such, chlorine must be added to the system continuously (43). The employees responsible for well maintenance failed to do this, allowing non-treated contaminated water to be consumed by the public, leading the to Walkerton Tragedy (17).

The Walkerton Tragedy is an example of the importance of proper water system maintenance; however, there are many other ways in which water may cause STEC related illness. Swimming in contaminated lakes or pools and washing vegetables with contaminated water are also ways in which individuals may become infected with STEC (43). Constant vigilance in maintaining the integrity of the water supply is necessary in order to prevent water-borne illnesses caused by STEC.

1.3.5.3 Animal Contact

Approximately 7-8% of STEC infections are caused by direct contact with animals (3). Individuals who often come into contact with livestock, through employment or visits to fairs where animals are present, are at higher risk for sporadic STEC infections (15, 26, 36). Petting zoos are the most common method of transmission implicated in animal contact outbreaks (44-46). Outbreaks related to petting zoos tend to result from lack of supervision and failure to emphasize the importance of proper hand washing (45). It is imperative that adequate hygiene facilities, such hand washing facilities, be made available where people are contacting animals. Eating areas are required to be located away from animal areas, and visitors must be closely supervised and also given proper instruction in hygienic practices (46).

1.3.5.4 Person-to-Person Transmission

Transmission of STEC from person-to-person is also a possible method through which the infection may be spread (47-51). This type of transmission occurs most often through the fecal-oral route, usually among children in day-care settings (18). In 2010, an outbreak in a

Colorado child-care center occurred resulting in 18 confirmed and 27 suspected cases of STEC related illness (18). Upon inspection, the site was found to have 3 critical health violations, which likely contributed to the spread of illness. Employees at this site repeatedly failed to wash their hands after diaper changes and before filling drink containers; disinfection procedures utilized were inadequate and food was consistently held at inappropriate temperatures (18). Another outbreak occurred among school children in France in 1992 that ceased only when Christmas holidays began, indicating the likelihood of person-person transmission (47).

Person-to-person transmission is most likely to occur in childcare facilities due to poor hand washing practices amongst children, overcrowding, and inadequate disinfection of diapering areas (48). In addition, symptomatic children often continue to attend the facility due to the lack of understanding of parents and staff of the implications of diarrhea (48).

In order to prevent secondary transmission of STEC, it is imperative that meticulous hygiene procedures be practiced (50, 51). To inhibit infection transmission, contact with symptomatic individuals must be limited, hand washing should be performed properly and often, food must be prepared carefully, and those individuals who are ill should stay home from work/school (50, 51).

1.3.6 Infectious Dose

The infectious dose of STEC has not yet been elucidated. Determining the infectious dose of STEC in humans is difficult, as one cannot ethically infect humans with doses of STEC in order to find the minimum infectious dose of the pathogen. An experiment by Tuttle *et al.,* found that the minimum infectious dose is likely less than 700 organisms by retrospectively examining the numbers of organisms present in lots of ground beef implicated in an outbreak (52). Likely, the infectious dose is less than 700 due to their experiments being conducted on raw ground beef while those who became ill consumed cooked ground beef,

which likely decreased the organism count (52). Further studies have estimated the infectious dose of STEC to be less than 100 organisms (53, 54).

1.3.7 Pathogenesis

1.3.7.1 Shiga Toxins Stx_1 and Stx_2

STEC produces two immunologically distinct forms of the shiga toxin – shiga toxin 1 and 2 (Stx_1 and Stx_2) protein (Figure 1-1). It is these toxins that cause the most severe manifestations of the disease such as hemolytic uremic syndrome. The research groups of Conrai and Neisser/Shiga independently discovered Stx_1 in 1903 as a toxin produced by *Shigella dysenterie* (55). In the case of non-*shigella* producers of shiga toxin, such as STEC, the toxin is more accurately known as shiga-like toxin. However, shiga toxin is the commonly used nomenclature for all forms of the toxin. Although the toxin is known formally as shiga toxin, it may also be referred to as verotoxin in reference to its toxic effect on vero cells (55). Shiga toxin 1, produced by STEC, differs from that produced by *S. dystenterie* by only 1 amino acid (56). Shiga toxin 1 and 2, produced by STEC, only share 56.8% amino acid sequence identity; however, despite this, they retain many similarities such as structure and mode of action (56-58).

X-Ray crystallography has played a key role in the elucidation of shiga toxin structure (55, 59). Both Stx_1 and Stx_2 belong to the AB_5 toxin group, and consist of a 32 kDa 'A' subunit and 40 kDa pentameric 'B' subunit, as shown in Figure 1-1 (55, 57, 58, 60, 61). The A subunit consists of an A_1 and A_2 chain linked by a loop containing 2 cysteine residues connected by a disulfide bond at positions 242 and 261 (55, 56, 60-62). The loop area contains a sequence of two arginine residues connected by 2 other amino acids that serve as an area of recognition for enzymatic cleavage (60, 62). A methionine residue in the A_2 chain serves to block the active site of the A_1 chain, preventing activation of the toxin until it reaches its destination and becomes enzymatically activated (60). The A_1 subunit is responsible for the catalytic activity of the toxin (61). The A_2 subunit is responsible for non-covalently linking the A subunit to the B by penetrating the central pore of the B pentamer (55, 56, 58, 61). The B subunit, responsible for

toxin binding and delivering the A subunit into the host cell cytoplasm, consists of a pentamer of five identical B chains (57, 60). Each B monomer making up the B subunit contains 3 binding sites for globotriaosylceramide (Gb3), the host cell receptor for shiga toxin (60).

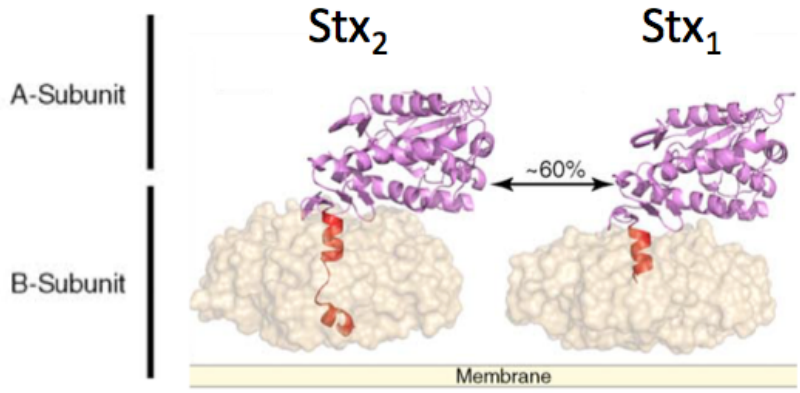

Figure 1-1. Structure of the AB_5 toxins, shiga toxin 1 (right) and shiga toxin 2 (left). The A_1 subunit is colored purple, the A_2 subunit red, and the B pentamer tan. The shiga toxin 1 and 2 proteins have 60% similarity (61). Reproduced with permission.

Although the structure of Stx_1 and Stx_2 are similar, there are a few key differences. The active site for Stx_2 remains accessible at all times versus that of Stx_1, which is blocked by a methionine residue from the A_2 chain until it is enzymatically cleaved within the host cell (58). The B chains that make up the B pentamer in Stx_2 are 2 residues longer than those of Stx_1 (58). In addition, the carboxy terminus portion of the A subunit in Stx_2 shows a slight alpha helix within the pore of the B subunit while the A subunit in Stx_1 shows no particular conformation (55, 58, 60).

Beyond structure, there are other key similarities and differences between Stx_1 and Stx_2. Both toxins have the same enzymatic function and are each encoded by an operon in which the A subunit gene lies proximal to that of the B subunit gene (55). Each toxin also shares the same eukaryotic cell receptor, globotriaosylceramide (Gb3) (with the exception of subtype Stx_{2e}, which binds

globotetraosylceramide (Gb4)) (55, 63). The A and B subunits also share the same role in toxin function and delivery. Some key differences in the two toxins involve regulation of gene expression, toxicity, and antigenicity. The *stx*$_1$ gene is repressed by iron while the *stx*$_2$ gene is not regulated by iron concentrations in the cell (55). The Stx$_2$ protein tends to be more toxic than Stx$_1$ and as such causes a more severe form of disease. It is suspected that the increased virulence of Stx$_2$ is due to Stx$_1$ being more likely to bind Gb3 in the lungs, while Stx$_2$ binds Gb3 in the kidneys (57). The toxins ability to bind the receptor also differs between the two toxins, and even among the Stx variants (55).

Shiga toxins 1 and 2 are not homogenous entities; variants/subtypes of these toxins exist (64-67). Seven subtypes of the *stx*$_2$ gene have been discovered, *stx*$_{2a}$, *stx*$_{2b}$, *stx*$_{2c}$, *stx*$_{2d}$, *stx*$_{2e,}$ *stx*$_{2f}$ and *stx*$_{2g}$ (64, 65, 67). Three subtypes of the *stx*$_1$ gene have so far been detected, *stx*$_{1a}$, *stx*$_{1c}$ and *stx*$_{1d}$ (64, 65, 67). The type of toxin and subtype has been associated with varying degrees of pathogenicity (66, 67). Stx$_{2d}$ appears to be less detrimental than other variants of shiga toxin 2 proteins, while Stx$_{2c}$ is more often associated with progression to serious clinical sequelae such as HUS (66, 67). Stx$_{2e}$ is associated with edema disease in pigs, rather than humans, and binds Gb4 rather than Gb3 (63, 67, 68). Stx$_{2f}$ has been isolated mainly from feral pigeons (67). Individuals infected with STEC that expresses Stx$_{2c}$ are much more likely to develop HUS, especially when Stx$_{2c}$ is expressed alone and not in combination with other Stx toxin subtypes (67). A 2002 study of 626 clinical isolates by Friedrich *et al.,* (67) detected *stx*$_2$ genes in 36% of the samples: 23.6% contained *stx*$_{2c}$ in combination with another toxin and 4.5% contained only *stx*$_{2c}$ (67). The *stx*$_1$ gene was detected in 26.5% of isolates (67). The heterogeneity of shiga toxins 1 and 2 illustrates the complexity of the toxin and plays a role in the degree of pathogenicity of the toxin.

The method used by the toxin to enter the host cell is dictated by its AB_5 structure. The B pentamer of the toxin recognizes the host cell receptor, which in the case of shiga toxin, is the glycosphingolipid Gb3 present in the host cell membrane (55-58, 60-62). Gb3 is expressed in the microvascular epithelium of

cells, primarily those of the kidney tubular epithelium (61). Once the B pentamer binds the host cell, the catalytic A subunit is endocytosed and transferred to the endoplasmic reticulum (ER) by retrograde transport via the golgi apparatus (60, 61). Once in the ER, the A subunit is unfolded by protein disulfide isomerase and transported into the cytosol where it refolds and causes cellular toxicity (61). Before the A subunit is moved to the cytosol, the A_1 and A_2 subunits are cleaved at a Arg-X-X-Arg sequence found within the loop between the disulphide linked cysteines by the protease furin (60, 62, 69). This cleavage dissociates the A_1 and A_2 domains, which exposes the A1 active site (60). The active A_1 domain consists of a N-glycosidase, which inhibits host cell protein synthesis by removing an adenine residue at position 4324 of the 28S rRNA (56-58, 60-62, 69). This prevents transfer RNA from binding and subsequent protein synthesis, resulting in cell death (57).

1.3.7.2 Enterohemolysins

Enterohemolysin production has been associated with STEC serotypes O157:H7, O26:H11, O103:H2, O111;H-, O113:H21, O5:H-, and O84:H2 (70). The *ehx* gene found on the pO157 plasmid encodes enterohemolysin, a pore-forming cytotoxin (70). The role of enterohemolysin remains unclear; however, there is speculation that it plays a role in lysing erythrocytes released during shiga toxin mediated bowel damage (1, 70, 71). Lysis of erythrocytes would result in the release of heme, which could serve as a source of iron for the pathogen (1, 71). Production of enterohemolysin occurs maximally under anaerobic conditions such as those found in the human bowel. Thus far the role of enterohemolysin disease development has remained un-elucidated; however, HUS patients are known to produce antibodies to the protein, indicating enterohemolysin likely does play a role in disease development (1). The role of enterohemolysin must be studied further, as its presence in a large number of STEC strains indicates it may play an important role in virulence.

1.3.7.3 Intestinal Adherence Factors

In the majority of illnesses caused by STEC, attaching and effacing (A/E) lesions, form on the gut mucosa resulting in damage to the intestinal lining (72-78). The process of pathogen attachment to the eukaryotic host cell causes these lesions (72-78). The main elements in pathogen attachment are intimin, encoded by the *eae* gene, and the translocated intimin receptor (TIR). Both the genes for intimin and TIR are found on the Locus of Enterocyte Effacement (LEE) pathogenicity island, which is chromosomally located (72-76, 78, 79).

Intimin is an outer membrane protein of 94-97 kDA in size, and thus far is the only adherence factor proven to play a role in intestinal colonization (73). Intimin is essential for attachment of STEC to the eukaryotic host cell, and displays a preference for attachment to the follicle-associated epithelium of Peyer's patches in the ileum (73). Nucleolin and β1 Integrin, eukaryotic host cell proteins for which intimin displays an affinity, are possible host cell receptors for intimin (72). Up to 17 variants of the *eae* gene have been discovered, with those producing intimin β1 being the most common (74). It is thought that different variants of intimin may result in varying degrees of affinity for host cells and tissues (74).

The LEE pathogenicity island carries many of the genes required for STEC attachment to host cells. In addition to genes for intimin and TIR, it also encodes the type 3 secretion system (T3SS) required for transporting TIR into the host cell as well as transcriptional regulators (73, 76). When STEC comes within close proximity of a potential host cell, the genes for TIR are upregulated (75). The T3SS injects TIR into the host cell where it incorporates itself into the intestinal epithelium (72). Intimin, on the outer membrane of STEC, recognizes TIR's intimin binding domain and binds TIR resulting in attachment to the host cell (72, 75). The combination of TIR and intimin then acts as a signal for actin assembly, forming a pedestal that more permanently anchors the bacterium to the host cell surface, resulting in A/E lesion development (72-75, 78). Therefore, the colonization genes located on the LEE pathogenicity island are necessary for full STEC virulence.

1.3.8 Disease Associated with STEC Infection

1.3.8.1 Presentation of Disease

STEC is responsible for a spectrum of illness that can range in severity from non-bloody diarrhea, to bloody diarrhea to hemolytic uremic syndrome (HUS) (1, 2, 80). STEC infections may present in a similar fashion to non-infectious disorders such as appendicitis, inflammatory bowel disease, and ischemic colitis (2). Typical illness caused by STEC infection progresses predictably, beginning with a period of stomach cramps, development of non-bloody diarrhea within 1-2 days and bloody diarrhea with severe abdominal pain within 2-4 days of onset (2). Typically the disease then resolves; however, complications such as colonic stricture, cholecystitis, colonic perforation, rectal prolapse, myocardial dysfunction and hemorrhagic cystitis may occur (1, 2). In some cases more severe disease may develop such as hemorrhagic colitis (HC) and HUS (1, 2, 4, 7, 42, 81-83).

Hemorrhagic colitis is characterized by severe abdominal pain, bloody diarrhea, and colonic mucosal edema/hemorrhage. Vomiting occurs in approximately 50% of patients and fever may or may not be present (80, 83-86). HC occurs as a result of damage to the intestines incurred during STEC infection. The pathogen binds to Peyer's patches in the ileum and colonization of the colon follows resulting in the induction of inflammation (80, 84). STEC virulence factors are activated resulting in A/E lesions and intestinal cell apoptosis due to toxin expression (80). During the course of colonization, the intestinal mucosa experiences a high degree of cellular injury resulting in hemorrhage and edema (Figure 1-2).

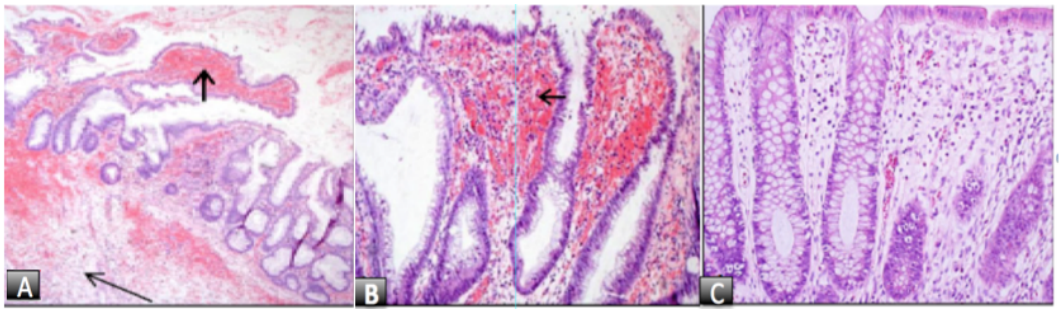

Figure 1-2: Intestinal pathology in a patient affected with STEC (A and B). Short arrows represent hemorrhages while long arrows represent intestinal infiltrates. A healthy control is represented by C (84). Reproduced with permission.

HUS occurs in approximately 10% of STEC patients under the age of 10 and is a major cause of renal failure in children (2, 81). The link between STEC infection and HUS was first discovered in Canada between 1983 and 1985 (82). HUS is caused by damage to the vascular endothelium of the kidneys and typically develops 1 week after the onset of diarrhea (2). HUS is associated with the triad of microangiopathic hemolytic anemia, renal failure and thrombocytopenia and presents with pallor, oligo/anuria and edema (1, 2, 7, 80-82, 87). HUS most commonly affects children; in the case of adults, disease tends to resemble thrombotic thrombocytopenic purpura (TTP) with neurological symptoms (2). Most patients who develop HUS fully recover; however, these individuals have up to a 30% chance of developing severe sequelae such as central nervous system impairments and renal impairment (1).

HUS develops primarily as a result of the action of shiga toxins, predominantly Stx_2, on the kidneys (42, 80, 87). Upon binding Gb3 receptors in the kidneys, shiga toxin causes damage to endothelial cells causing nephron loss, endothelial dysfunction, and capillary wall thickening (42, 87). Damaged endothelial cells detach from the basement membrane resulting in vasoactive substance production and collagen exposure (80, 87). Circulating platelets are activated by contact with shiga toxin and vasoactive substances produced by damaged cells and bind to exposed collagen. Aggregation of platelets on the endothelium results in the accumulation of fibrin thrombi in the microvasculature, hindering blood flow as well as an overall thrombocytopenia (80, 87). As red

blood cells travel through the fibrin-clogged microvasculature, they become damaged, which is indicated by the presence of schistocytes (fragmented red blood cells) on a peripheral blood smear and free hemoglobin in the plasma. Damaged red cells are then removed by the reticuloendothelial system resulting in anemia, in this case microangiopathic hemolytic anemia (MAHA) (80, 87). Occluded vessels compromise blood flow to the kidneys and other organs, resulting in further cell death and ultimately renal failure (87). Neurological impairment may also occur as neurons also express Gb3; however, this is more common in adults than children (80).

1.3.9 Prognosis

The prognosis of STEC infection is good; most infected individuals recover completely and develop no sequelae (1). However, in the 10% of cases that develop HUS, 3-5% mortality occurs and up to 30% experience severe sequelae such as renal failure, hypertension and central nervous system impairment (1, 87). A 2010 study of nearly 2000 individuals by Clark *et al.,* found that 4 years after the Walkerton STEC outbreak, STEC victims had a 25% increase in risk for hypertension, were 3x more likely to experience some form of renal impairment and 2x more likely to develop cardiovascular problems (42).

1.3.10 Treatment Methods

Treatment of STEC infections is generally limited to supportive care, such as IV rehydration, renal dialysis, and blood transfusions (1, 2, 88, 89). Fluid and electrolyte levels must be maintained to prevent volume depletion and reduce stress on the kidneys, which will reduce the chance that dialysis will be required (2, 88, 89). Dialysis may be necessary if the patient becomes severely acidotic (to the point that correction with medication is impossible), hyperkalemic, or experiences severe edema (89). Hemoglobin, hematocrit and platelet count must be carefully monitored to assess the need for transfusions (88). At this time, antibiotics are not recommended as killing the organism will result in the release of more toxin into the patient's system, increasing the chance of severe complications such as HUS (2, 88). Antimotility agents are to be avoided, as they

will decrease clearance of the organism, increasing the likelihood of HUS (1, 2). Studies have been done using Gb3 analogues, which preferentially absorb the toxin, and shiga toxin neutralizing antibodies; however, limited success has been reported and supportive therapy remains the treatment of choice (1, 88).

1.4 Current Diagnostic Methods for STEC

1.4.1 Specimen Collection

The ideal specimen for STEC testing is a diarrheal stool sample collected directly after the onset of symptoms and before initiation of treatment (7). The sample should be collected in a sterile container and sent to the microbiology laboratory as soon as possible. Once the sample arrives in the laboratory, processing should occur at the time of receipt (7). If immediate processing is not possible the sample should be refrigerated for a maximum of 24 hours if the sample is unpreserved or 48 hours if the sample was collected in transport medium (7).

1.4.2 Current Methods of STEC Detection

1.4.2.1 Culture

Historically, STEC has been detected using culture-based methods, specifically Sorbitol MacConkey (SMAC) agar (7, 90, 91). SMAC is similar to traditional MacConkey agar; however, SMAC contains sorbitol in place of lactose (91). As STEC O157 is unable to ferment sorbitol in SMAC agar, O157 colonies appear colorless, while any bacteria that are able to utilize sorbitol appear pink (90, 91). As *E. coli* O157 is the only STEC that is unable to ferment sorbitol, other STEC will appear pink on SMAC and thus not be differentiated from commensal *E. coli* (7, 90, 91). It has been estimated that between 28 and 52% of all STEC infections are caused by non-O157 STEC, therefore using SMAC alone results in missing up to 50% of STEC infections (90).

In recent years, new culture-based methods for detecting STEC have been developed; however, these have not yet been adopted as

mainstream testing methods. Chromogenic agars, such as BBL CHROMagar O157 (BD, Mississauga, Ontario), detect O157 using chromogenic substrates used by *E. coli* in the media (92-94). These new chromogenic methods have similar sensitivities to SMAC for O157 detection but do not reliably detect non-O157 STEC (92, 94). CHROMagar STEC (CHROMagar, Paris, France) is another chromogenic culture media for STEC detection upon which O157 STEC grows as non-fluorescing mauve colonies and non-O157 STEC appears as mauve colonies that do fluoresce under UV light (95, 96). Independent studies by Wylie *et al*., and Gouali *et al*. found that CHROMagar STEC was able to support the growth of many serotypes of STEC; however, some non-STEC organisms were able to grow on and in certain cases failed to support growth from shiga toxin positive stools (95, 96). These results indicate that CHROMagar STEC may be useful as a supplemental media but is not suitable to be used as a primary media STEC detection as confirmatory tests such as PCR or EIA are still required (95, 96).

1.4.2.2 Enzyme Immunoassay

Immunoassays detect free shiga toxin produced by STEC in stool, and have the advantage of being able to detect all serotypes of STEC that produce shiga toxin (7). Enzyme immunoassay (EIA) was first licensed for diagnostic use in 1995, and has since been recommended by the CDC as a method for detecting STEC (7, 90). Immunoassays used for detection of STEC include Premier EHEC (Meridian Bioscience Inc., Cincinnati, OH), Immunocard STAT! EHEC (Meridian Bioscience Inc., Cincinnati, OH), and Duopath Verotoxins Gold Labelled Immunocard Assay (Merck) (7). Advantages of immunoassays include their speed (as compared to culture) and ability to detect all serotypes of STEC. Disadvantages are their inability to differentiate among the STEC serotypes beyond whether they produce Stx_1 or Stx_2, the labour intensive nature of the assay and the need for parallel culture to further characterize isolates (97).

1.4.2.3 PCR

Currently, both conventional and real-time (RT) PCR are used to detect STEC (7). Nucleic acid testing is advantageous in that primers can be designed to detect any desired gene such as *stx*$_1$, *stx*$_2$, O group genes, and *eae* (7). Generally in clinical laboratories, PCR is performed using DNA extracted from stool samples enriched in MacConkey Broth. If positive results are obtained, the stool sample is plated onto selective isolation media and suspect colonies are then picked for testing. Colonies are picked for testing based upon their appearance on the media (e.g. clear colonies on SMAC). Although in theory any combination of genes can be tested for using PCR, in practice only the *stx*$_{1/2}$ genes are amplified and positive isolates (those testing positive for *stx*$_1$ and/or *stx*$_2$ genes) are sent for serological testing to determine the serogroup of the isolate. Although conventional and RT-PCR are highly sensitive and specific methods of *stx* detection compared to culture, the high cost of equipment, dedicated workspaces and trained personnel required for these assays limits their use to dedicated molecular diagnostic laboratories (7).

1.4.3 Laboratory Testing in Areas of Limited Resources (AOLR)

Current methods of STEC testing are not well suited to areas of limited resources (AOLR) such as developing nations or remote isolated communities in northern Canada. In 2004, the World Development Report cited lack of access and unaffordability of laboratory tests as the main reason why laboratory initiatives fail in developing nations (98). Such areas are unable to purchase and maintain the equipment required for current molecular methods such as PCR and lack the infrastructure needed to facilitate timely delivery of supplies (8, 99, 100). As such, molecular testing has not yet been considered a viable option for AOLR (100).

Poor access to reliable laboratory testing has resulted in physicians relying solely on their clinical judgment to make diagnoses, with no possibility of confirming their decisions with laboratory data (8, 101). This lack of information

leads to delayed and missed diagnoses as well as inappropriate and ineffective treatments (8). In an effort to improve the quality of laboratory testing in AOLR, in 2001 the Sexually Transmitted Disease Diagnosis Initiative of the World Health Organization created the ASSURED criteria for laboratory tests (98, 100). The ASSURED criteria states that laboratory tests for AOLR should be **A**ffordable, **S**ensitive, **S**pecific, **U**ser-friendly, **R**apid and robust, **E**quipment free, and **D**eliverable (98, 100). These criteria ensure that assays designed for use in AOLR will be reliable, inexpensive, and simple to perform.

1.5 Loop Mediated Isothermal Amplification (LAMP)

1.5.1 Introduction to LAMP

LAMP was developed in 2000 by a team led by Notomi T *et al.,* of Eiken Chemical in Japan (102). The LAMP method synthesizes DNA through the principles of strand displacement, and accordingly utilizes the enzyme *Bst* polymerase, which has a high strand displacement activity (102). The assay is simple to perform and involves only heat denaturation of the sample DNA in the reaction mixture, cooling the sample on ice to prevent the DNA strands from reannealing, adding enzyme, and running the reaction for approximately 1 hour at 65°C (102). Results are then visualized using agarose gel electrophoresis. Based on the simplicity of performing LAMP there is great potential for the LAMP assay to be used in AOLR and as a rapid detection assay.

1.5.2 LAMP Primer Design

The first LAMP reactions utilized a total of 4 primers, 2 inner primers (FIP and BIP) and 2 outer primers (F3 and B3) (102). In 2002 the LAMP reaction was further improved by the addition of two loop primers (LF and LB) (103). As seen in Figure 1-3, the inner and outer primers correspond to 6 regions of the template strand (F1c, F3, B2, B1c, F3 and B3), which ensures a high degree of specificity (102). The forward inner primer (FIP) consists of the F1c region of the template linked to the F2 region by a TTTT spacer, the backward inner primer (BIP) consists of the B2 region linked to the B2c region by a TTTT spacer (102). The

forward outer primer (F3) and the backward outer primer (B3) correspond to the F3 and B3 regions of the template respectively.

When assigning regions to the template sequence it is recommended that the software PrimerExplorer be used (104). This software will both assign regions to the template sequence and generate primer sets according to default criteria. To design LAMP primers, the distance between primer regions, melting temperature, and secondary structure must be taken into account. According to Eiken Chemical, the distance between the 5' ends of the F2 and B2 regions should be 120-180 bp, the distance between F2 and F3 (B2/B3) should be 0-20 bp and the 5' end of F2 (B2) should be 40-60 bp from the 3' end of F1 (B1) (105). The optimal melting temperature of F2 and B2 in the template sequence has been determined to be between 60 and 65°C, which is within the optimal working temperature of *Bst* polymerase (102, 105). The melting temperature of F1c/B1c is slightly higher which helps ensure that looped structures are formed after the release of single stranded DNA from the template sequence (102). The melting temperatures of F3/B3 are lower than F1c/B1c order to ensure that the inner primers take part in the reaction before the outer primers (also guaranteed by the outer primers being present in approximately 1/10 the concentration of the inner primers) (102). To prevent false positive amplification, secondary structure formation must be avoided (105). Formation of secondary structure can be avoided by ensuring the 3' end of the template is not AT rich or complementary to other primers (105).

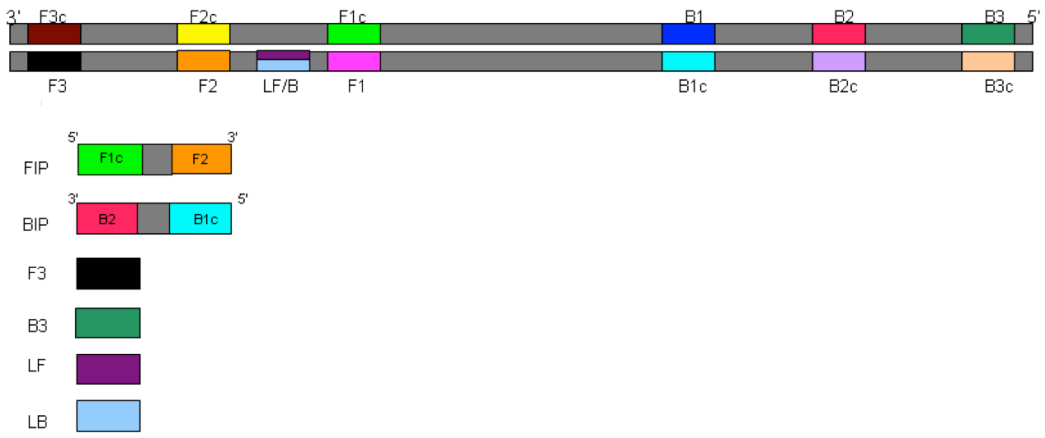

Figure 1-3: LAMP primer design. The template DNA strand is represented in grey with specific regions of template indicated by colored boxes. LAMP primers are represented below the template strand, loop primers: LB (light blue), LF (purple); outer primers: B3 (dark green), F3 (black) and inner primers: BIP (pink linked to cyan) and FIP (light green linked to orange) (105).

1.5.3 *Bst* Polymerase

Bst polymerase is a 76 KDa DNA polymerase derived from *Bacillus stearothermophilus* (106, 107). This enzyme has 5'-3' exonuclease activity but lacks the 3'-5' exonuclease required for proofreading activity (106). The optimal reaction temperature for *Bst* polymerase is between 55-65°C (107). At temperatures above 70°C, enzyme activity is significantly decreased while at 80°C the enzyme is inactivated (107).

1.5.4 LAMP Mechanism

The LAMP mechanism can be separated into 3 main phases as shown in Figure 1-4, (i) the starting material production step, (ii) the cycling step and (iii) the elongation/recycling step (102). Each of these steps will be explained in turn. Although the mechanism is complicated, reaction setup is simple and involves only adding enzyme to a solution of reaction mixture and denatured template, and running at a single temperature for a specified period of time.

The purpose of the starting material production step is to produce the barbell-like structure indicated by structure 6 in Figure 1-4 (102). The FIP, which is present in the highest concentration, is the first to bind the target DNA (102).

The F2 portion of the FIP binds the F2c region of the target DNA and initiates synthesis of a complementary strand in the presence of *Bst* polymerase. F3 enters the reaction after synthesis of the complementary strand by FIP and binds the F3c region on the template strand (102). As the F3 primer begins synthesis of a new strand, the complementary strand produced by the FIP primer is displaced from the template (102). The FIP remains linked to the complementary sequence and a loop is formed as the F1c region on the primer binds to the F1 region on the complementary strand, as seen in Figure 1-4. The FIP-linked complementary strand becomes the template for the BIP and B3 primers resulting in the formation of a dumbbell structure, which is the starting point for LAMP cycling and elongation (102).

Once the dumbbell-like structure is formed, the F3 and B3 primers are depleted and no longer participate in the reaction (102). The F2 region of the FIP primer binds the F2c region found in the loop of the starting structure and begins synthesizing a new strand, leading to the generation of a stem-loop DNA with one gap and a formation of another loop at the opposite end of the sequence as depicted by structure 8 in Figure 1-4 (102). Continuous FIP primed strand displacement DNA synthesis leads to multiple stem-loop structures with constantly elongated stems and loops on one end (102). These FIP generated produced are the templates for BIP primed strand displacement synthesis, leading to a 3x amplification of the target sequence at every half cycle. This process continues until the reaction is terminated and results in the production of stem loop DNA structures with a variety of stem lengths and number of loops (102).

Loop primers may also be added to the LAMP reaction to increase efficiency of DNA amplification (103). The loop primers (LF/LB) bind the stem loops not already bound by the inner primers and initiate further strand displacement DNA synthesis (103). As the loop primers bind loop structures, they do not participate in the reaction until structure 6 in Figure 1-4 (102). LF and LB bind between the F3 and F1 (B1 and B2) regions in the DNA sequence. With the

addition of loop primers, all loop structures are bound and reaction rate increases (103).

Template DNA size is a critical factor in the efficiency of the LAMP reaction, as the reaction is limited by the time it takes for strand displacement to occur (102). Templates should be between 130 and 200 bp in size for optimal amplification. Templates greater than 500 bp are too large for strand displacement to occur efficiently and will result in poor amplification (102). Betaine is added to the reaction in order to destabilize the DNA helix and negates the need for heat denaturation of the template (108). It is theorized that reaction temperatures of 65°C in conjunction with betaine are sufficient to facilitate strand separation; however, the exact mechanism is unknown (108).

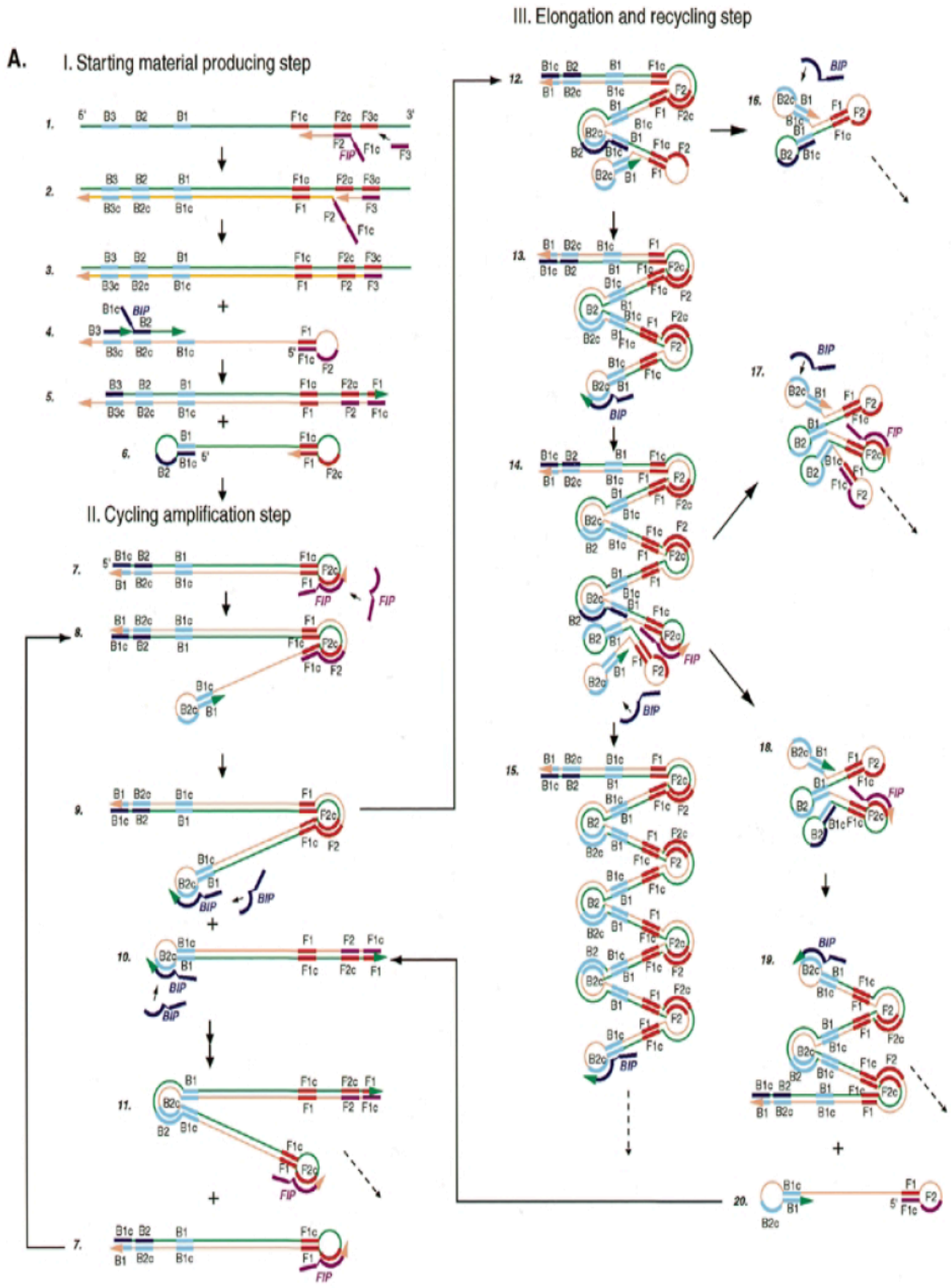

Figure 1-4: LAMP mechanism (102). Reproduced with permission.

1.5.5 Product Detection

As with conventional PCR, LAMP products can be visualized using agarose gel electrophoresis followed by visualization under UV light. In this process, an electric current is applied to an agarose gel with wells containing the LAMP DNA product. The LAMP DNA migrates along the gel towards the cathode, and the products separate based upon size, with smaller fragments travelling the farthest towards the cathode. Ethidium bromide in the gel binds the DNA and will fluoresce under UV light wherever DNA is present. Positive LAMP results are indicated by a ladder-like product. This ladder-like product is due to the many sizes of amplification products generated by the reaction. Traditionally, this is the method of detection used for LAMP products; however, due to the cost and equipment required, other methods such as turbidity, and fluorescent dyes have been explored.

In 2001, Mori *et al.,* discovered that LAMP products could be detected using either a spectrophotometric method or in some cases, even the naked eye (109, 110). This characteristic of the LAMP reaction is possible due to the large amount of DNA produced by the reaction, relative to other assays such as the polymerase chain reaction (109, 110). In LAMP, pyrophosphate ions are produced in large amounts during DNA polymerization and form a precipitate with magnesium ions found in the buffer solution, forming magnesium pyrophosphate. This is demonstrated by the reaction equation (109):

$$(DNA)_{n-1} + dNTP \rightarrow (DNA)_n + P_2O_7^{4-}$$

$$P_2O_7^{4-} + 2Mg^{2+} \rightarrow Mg_2P_2O_7 (109)$$

The precipitate produced was confirmed to be magnesium pyrophosphate through infrared spectroscopy and chemical analysis (109). The precipitate is produced in a linear fashion according to reaction progression and measurable at 650 nm using a spectrophotometer (110). In many cases the authors found that the turbidity could be seen by the naked eye following centrifugation of the sample to bring the precipitate to the bottom of the tube (109). In order to get sufficient production of magnesium pyrophosphate for visual analysis, at least 4 µg of DNA must be produced during the reaction (109). LAMP reactions tend to

produce approximately 10 µg of DNA per 25 µL reaction, whereas conventional PCR results in only 0.2 µg of DNA per 25 µL reaction, accounting for the observation that visual turbidity is seen only with LAMP reactions (109). As this method relies on production of a precipitate, it is unsuitable for samples that are turbid or contain impurities that absorb in the same range as magnesium pyrophosphate (109).

Hydroxynaphthol blue is a metal ion indicator that can be used to detect Ca^{2+} under conditions of pH 13 or Mg^{2+} at pH 10 (111). As the LAMP reaction proceeds at pH 8, Goto *et al.,* hypothesized that hydroxynaphthol blue could be used to monitor the change in magnesium ion concentration as the reaction progresses (111). Addition of 120 µM hydroxynaphthol blue prior to amplification produced a visible color change in positive reactions that could be measured spectrophotometrically at 650 nm (111). Negative samples appeared violet due to free Mg^{2+} being present in the reaction; however, positive samples appeared sky blue due to Mg^{2+} being bound by pyrophosphate. This method is advantageous over other methods as the dye can be added pre-amplification without causing inhibition of the reaction, which decreases the risks of false positives occurring from aerosolization (111). A 2010 study by Wastling *et al.,* showed that hydroxynaphthol blue can be a valuable method of product detection; however, inter-reader variability in the detection of endpoints by the naked eye can be subjective (112).

Other metal ion indicator systems have been used to identify LAMP products, such as the calcein/manganese system developed by Tomita *et al.,* (113). This system takes advantage of the change in metal ion concentration throughout amplification process for detection of amplification products (113). Initially, calcein (a fluorescent metal ion indicator) is bound by manganese ions in the reaction and thus is unable to produce a fluorescent signal. As the reaction progresses, pyrophosphate ions are produced, which preferentially bind the manganese ions, leaving calcein unbound (113). The unbound calcein produces a fluorescent signal that is strengthened when it binds free magnesium ions in

the solution. The fluorescence produced by positive samples is observable under UV illumination, while negative samples produce no fluorescence (113).

Sybr Green I is a dye that when bound to double stranded DNA produces a fluorescent signal that can be detected both by visible and UV light (114). When intercalated with dsDNA produced by LAMP, the reaction turns green and fluoresces under UV light; when unbound to dsDNA, the reaction is orange and does not fluoresce (115-117). Sybr Green I is approximately 6-8x more sensitive than ethidium bromide and has the added benefit of not being carcinogenic (116). Sybr Green I inhibits the LAMP reaction and thus cannot be added pre-amplification; however, adding the dye post-amplification necessitates the opening of the reaction tubes which increases the risks of contamination through aerosolization of amplicons (115, 117). A benefit of using Sybr Green I is the longer-term stability as compared to other reagents such as calcein which have shorter shelf lives (117).

1.5.6 Equipment Requirement

Most nucleic acid testing methods such as conventional and RT-PCR require expensive and complicated equipment such as thermocyclers or RT-PCR platforms, such as the ABI Prism® 7500 FAST (Applied Biosystems, Foster City, California USA). As LAMP is an isothermal reaction, it requires only simple equipment such as a water bath or heat block (102). Any apparatus capable of holding samples at the constant temperature required for the reaction can be used.

1.5.7 Advantages of the LAMP Method

The LAMP method has many advantages over other methods of nucleic acid amplification. LAMP is highly sensitive and specific due to the 6 areas on the target sequence that the primers must bind (102). LAMP is a robust method that is less affected by the presence of inhibitors than conventional PCR, making DNA purification less vital (118, 119). The multitude of possible detection methods make LAMP a versatile method that can be tailored to the resources available in a particular laboratory (119). The simplicity and cost effectiveness of

LAMP make it an ideal method for nucleic acid amplification, both in developed and developing countries.

1.5.8 Disadvantages of the LAMP Method

The main disadvantage of LAMP over other assays, such as conventional PCR, is that LAMP amplification products are ‘non-specific’, as all LAMP products look the same and thus cannot be discriminated based on size. The identity of the LAMP product cannot be determined by looking at a gel and comparing with a DNA ladder as can be done with conventional PCR (112). The ladder-like product obtained with LAMP looks the same, even when different primer sets are used, hence one must assume that due to LAMPs highly specific nature, positive results are due to amplification of the intended target (112). LAMP is not a quantitative, but a qualitative assay, and as such there is no indication of yield. In addition, the high amplicon yield seen with LAMP increases the possibility of contamination due to amplicon aerosolization when tubes are opened post-amplification (117).

1.5.9 LAMP in Areas of Limited Resources

Most nucleic acid testing methods, such as conventional or real-time PCR, do not meet the WHOs ASSURED criteria for laboratory testing in areas of limited resources due to their cost and complexity (119). LAMP however, does have potential to be used as a rapid diagnostic test in developing areas as it does not require expensive equipment or reagents and is relatively rapid (118). LAMP has the potential to be incorporated into closed-tube systems where amplification results can be visually detected. The multiple detection methods possible enable some ability to tailor the assay to the laboratory and environment it will be used (118). The robustness of LAMP when faced with the presence of inhibitory substances makes DNA purification less vital and thus decreases the cost and time due to sample processing (118). All of these characteristics make LAMP a possible method of bringing molecular diagnostic testing to areas of limited resources.

1.6 Research Rationale

Currently, the majority of molecular laboratories detect STEC virulence genes (*stx*$_1$ and *stx*$_2$) in clinical stool samples using real-time PCR (RT-PCR). RT-PCR is not an ideal method as it requires highly technical equipment such as the ABI Prism® 7500 FAST (Applied Biosystems, Foster City, California USA) which prevents its use in areas of limited resources. The development of a simple to perform, cost-effective method of *stx* gene detection would allow smaller and/or more remote laboratories to test for these genes and thus increase test turn-around-time and improve patient outcome. Loop-mediated isothermal amplification is an assay that has the potential to bring molecular testing for *stx* genes to all laboratories regardless of their size or location.

1.6.1 Hypothesis

Loop-mediated isothermal amplification (LAMP) represents an inexpensive, simple to perform method of testing for STEC virulence genes, *stx*$_1$ and *stx*$_2$ in clinical stool samples. When compared to current testing methods such as RT-PCR, LAMP equals or exceeds the ability of RT-PCR to detect *stx*$_1$ and *stx*$_2$ in clinical stool samples in terms of cost-effectiveness, sensitivity, specificity and turn-around-time. Sybr Green I visual detection of LAMP products eliminates the agarose gel electrophoresis product detection step thus increasing the simplicity and cost-effectiveness of the assay.

1.6.2 Objectives

The objectives of the study were divided into 4 main parts:

(1) To determine the optimal reaction conditions for a loop-mediated isothermal amplification reaction (LAMP) using a set of previously published *stx*$_1$ and *stx*$_2$ primers.

(2) To compare the performance of the optimized LAMP reaction to conventional PCR and the current gold standard, real-time PCR, in terms of cost, sensitivity, specificity and turn around time.

(3) To evaluate the optimized LAMP reactions for use with clinical stool samples and compare these results to those previously obtained by real-time PCR.

(4) To develop an alternative method of product detection using Sybr Green I in an attempt to eliminate the need for agarose gel electrophoresis product detection.

Chapter 2: Background

2.1 Optimization of a loop-mediated isothermal amplification for the detection of Shiga-toxin producing *Escherichia coli* and Comparison to Current Diagnostic Methods

Numerous methods for nucleic acid amplification testing have been developed; however, this thesis will focus on loop-mediated isothermal amplification (LAMP) due to its relatively recent development and possible applications to laboratory testing in areas of limited resources. Currently, *stx* genes can be detected using conventional PCR, or real-time PCR. These current methods are expensive and time consuming. LAMP represents a method that requires little equipment or expertise to perform, which will make molecular testing accessible to all clinical microbiology laboratories.

The first step in assay implementation, after primer design, is optimization. Optimization ensures the assay is performing at its peak sensitivity and specificity by determining the optimal concentrations of reagents and reaction conditions for amplification.

The LAMP reaction for the detection of STEC will be optimized using primer sets for stx_1 and stx_2, developed by Hara-Kudo *et al.,* and compared to conventional and real-time PCR (120). The LAMP reaction will be optimized for temperature and time, as well as concentrations of magnesium sulfate and enzyme. Finally, comparisons will be made based upon sensitivity, specificity, turn-around-time and cost.

2.2 Application of the Optimized LAMP Reaction to Clinical Samples

Currently, STEC is detected in clinical samples using culture-based methods, enzyme immunoassay or nucleic acid amplification systems (121). As less than 100 organisms of some STEC serotypes are sufficient to cause severe disease, detection methods must be robust and sensitive (121). Traditional culture methods have long turn-around-times and tend to under-diagnose non-O157 STEC serotypes, while EIA methods are susceptible to false positives and negatives (121). Nucleic acid amplification methods, such as PCR, have shown

great promise for STEC detection; however, inhibitors found in clinical samples tend to decrease the ability of these methods to detect *stx* genes. In addition, the high cost of equipment associated with molecular methods limits their implementation in many laboratories (121-123).

LAMP is a promising method of detecting STEC in clinical samples as it is considered to be less susceptible to inhibitory substances such as hemin, whole blood, anticoagulants, n-acetyl cysteine and sodium chloride than conventional PCR or RT-PCR (122). In addition, LAMP tends to be more sensitive, specific, cost-effective, and simpler to perform than more traditional molecular methods such as conventional PCR and RT-PCR (121-124).

The optimized LAMP assay will be tested using DNA extracted from clinical stool samples by a rapid lysis method. Results obtained by LAMP will be compared to those previously obtained from the same clinical samples using RT-PCR.

2.3 Development of a Visual Detection Method for LAMP

Although LAMP shows promise as a simple, cost effective method of DNA amplification, the current agarose gel electrophoresis method of product detection complicates the assay by requiring specialized equipment, increasing turn-around-time (TAT), as well as the cost of the assay. Eliminating the agarose electrophoresis step would make LAMP more desirable as it would significantly decrease assay TAT and cost, as well as making the assay more user-friendly and portable.

Multiple options for eliminating electrophoresis have been examined in previous studies such as hydroxynaphthol blue, calcein, PicoGreen, and turbidity (111-113, 115, 116, 125-127). Many studies have found turbidity to be an unsatisfactory method of (111) product detection, as the amount of turbidity produced by a positive reaction has not been substantial enough for detection by the naked eye, thus necessitating the use of a turbidimeter (112, 119, 122, 126). Hydroxynaphthol, a metal ion indicator used for LAMP product detection by Goto *et al.*, was investigated as a possibility for use in this study; however, preliminary

results showed that a spectrophotometric reader would be required as differences between positive (sky blue) and negative (violet) results were not always immediately obvious to the naked eye (111). The goal of this part of the study was to eliminate the need for costly equipment for product detection, and rely solely on visualization by the naked eye. Hydroxynaphthol blue and turbidity were not considered options as these methods require the use of spectrophotometers or turbidimeters (112). Sybr Green I was investigated as a possible indicator for this study as previous work has shown it to produce more obvious results than other indicators, is easy to attain, stable at room temperature and cost effective (112, 115, 116, 125).

A visual detection method for LAMP products will be developed using the fluorescent dye Sybr Green I (SG1). The optimal reaction conditions using SG1 with LAMP will be determined and tested with DNA extracted from clinical stool samples, and results compared to those previously obtained by RT-PCR in Chapters 2 and 3.

2.4 LAMP Using a Commercial System

Due to the growing popularity and awareness of the LAMP assay, several options for assay automation have been developed. The first automated LAMP reader was Eiken Chemical's Loopamp Real-time Turbidimeter (128). In this study, a more recently developed instrument for performing the LAMP assay was evaluated – the Optigene Genie II. The Genie II measures real time fluorescence produced by positive reactions as well as annealing temperatures for further confirmation of the presence of amplified product (Optigene, Horsham, West Sussex, UK) (129).

There are many advantages to using an automated LAMP system such as the Genie II. Generally, these systems are small and easily portable which facilitates their use in multiple locations. The Genie II further facilitates this by including an internal rechargeable battery that allows it to be used in areas without access to electricity (129). The major advantage presented by automated

instruments is that reactions take place in a closed tube, which decreases the likelihood of contamination and therefore, false positive results.

Although there are many advantages to automated LAMP systems, there are also many inherent disadvantages. Often the equipment required to perform the assay with an automated system will be specific to the particular reader, therefore the user must rely on consumables produced by the company and cannot use generic supplies thus increasing cost. The instrument may also be limited to running a small number of reactions at a time (8 in the case of the Genie II), preventing the user from being able to set up large runs, which may increase the turn-around-time for results. In addition, the cost of the instrument system itself may be prohibitive for many smaller laboratories.

In this study, the Optigene Genie II was evaluated with DNA from the blinded clinical sample panel used previously and compared to results obtained with both the manual LAMP method and RT-PCR.

Chapter 3: Materials and Methods

3.1 Culture and Organisms Used

A panel of bacteria strains (see section 2.2.7) was selected from the Provincial Laboratory for Public Health (ProvLab) culture collection in Edmonton, Alberta, Canada. Bacteria strains were stored in vials of skim milk at -70°C. Bacteria were inoculated onto sheep blood agar plates (BAP) and incubated 18-24 hours aerobically at 37°C. All strains were further subcultured twice before performing experiments. For the optimization study, the Sakai strain (from the ProvLab collection), a well characterized STEC O157:H7 positive for both shiga toxin (*stx*$_1$ and *stx*$_2$) genes was chosen as the control strain to be used for the optimization.

3.2 DNA Extraction

DNA was extracted from overnight culture (aerobic, 37°C) using the 200 µL MagaZorb™ protocol (Promega, Madison, Wisconsin, USA) on the KingFisher nucleic acid extractor (Thermo Scientific, Ashville, North Carolina, USA). In this extraction procedure, a combination of proteinase K and lysis buffer causes DNA to be released (130). The DNA is then bound to MagaZorb™ magnetic beads in the presence of binding buffer, which are then captured by magnetic rods in the KingFisher extractor (130). Contaminants are removed from the magnetic bead solution using a wash buffer and the elution buffer is then used to elute the DNA from the beads (130). The extraction procedure was carried out as per manufacturer's instruction. DNA extractions were stored at 4°C if they were to be used immediately or at -70°C for later use.

3.3 Primers and Primer Reconstitution

Three sets of previously established *stx*$_1$ and *stx*$_2$ primers were used for this study (120, 131, 132). Figure 3-1 shows a schematic diagram of the location of the LAMP primers. Primer and probe locations for all 3 assays on the *stx*$_1$ and *stx*$_2$ genes are shown in Figure 3-1, primer sequences and references are listed in Table 3-1; primers were synthesized by Integrated DNA Technologies

(Coralville, Iowa, USA). Probes were synthesized by Applied Biosystems Custom Oligo Synthesis Service (Foster City, California, USA).

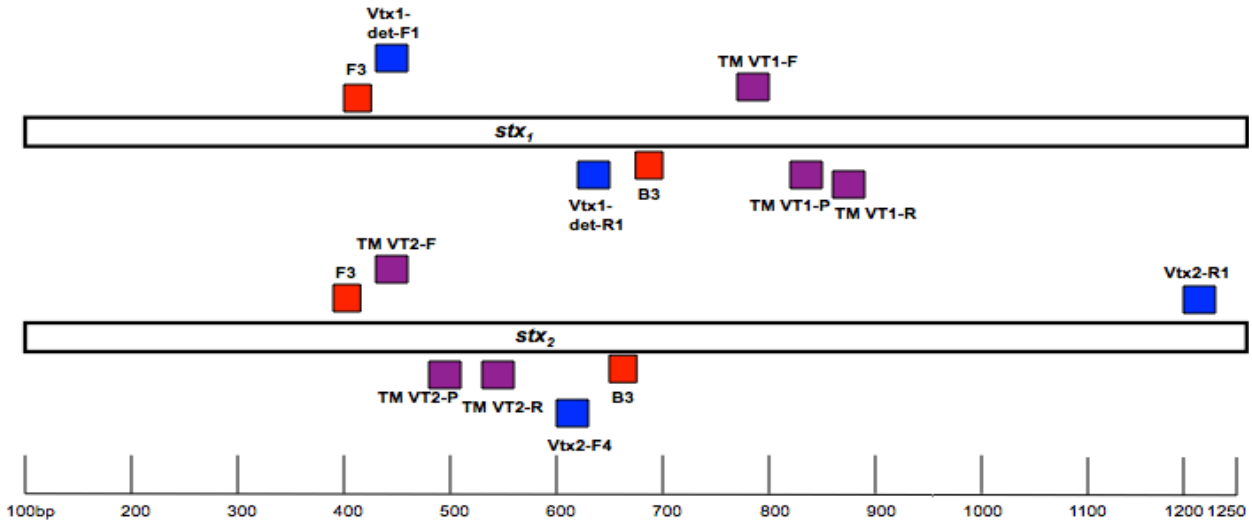

Figure 3-1: Schematic of LAMP (F3, B3), conventional PCR (Vtx1-det-F1/R1, Vtx2-F4/R1) and real-time PCR (TM VT1/2-F/R/P) primers and probe in relation to *stx*$_1$ and *stx*$_2$ loci. Only the F3 and B3 LAMP outer primers are represented as these represent the boundaries of the gene amplified by the LAMP primer sets. Conventional PCR primers for Vtx2-F4/f and Vtx2-R1-e/f are not shown, as they are located at the same position on the template strand as Vtx2-F4 and Vtx2-R1 respectively. Red, blue and purple boxes represent primers for LAMP, conventional PCR and RT-PCR respectively (120, 131, 132).

Table 3-1: Primers and Probes used for LAMP, Conventional PCR and Real-time PCR

Assay/Gene Target	Primer Name	Sequence 5'-3'
LAMP *stx*$_1$ Hara-Kudo *et al.* (120)	FIP	GCT CTT GCC ACA GAC TGC ACA TTC GTT GAC TAC TTC TTA TCT GG
	BIP	TGA CAG CTG AAG CTT TAC GCG AAA TCC CCT CTG AAT TTG CC
	F3	GCT ATA CCA CGT TAC AGC GTG
	B3	ACT ACT CAA CCT TCC CCA GTT C
	LF	AGG TTC CGC TAT GCG ACA TTA AAT
LAMP *stx*$_2$ Hara-Kudo *et al.* (120)	FIP	GCT CTT GAT GCA TCT CTG GTA CAC TCA CTG GTT TCA TCA TAT CTGG
	BIP	CTG TCA CAG CAG AAG CCT TAC GGA CGA AAT TCT CCC TGT ATC TGC C
	F3	CAG TTA TAC CAC TCT GCA ACG TG
	B3	CTG ATT CGC CGC CAG TTC
	LF	TGT ATT ACC ACT GAA CTC CAT TAA CG
	LB	GGC ATT TCC ACT AAA CTC CAT TAA CG
RT PCR *stx*$_1$ Chui *et al.* (131)	Taqman VT1-F	CAT CGC GAG TTG CCA GAA T
	Taqman VT1-R	GCG TAA TCC CAC GGA CTC TTC
	Vt_1Probe	6FAM-CTG CCG GAC ACA TAG AAG GAA ACT CAT CA-TAMRA
RT PCR *stx*$_2$ Chui *et al.* (131)	Taqman VT2-F	CCG GAA TGC AAA TCA GTC
	Taqman VT2-R	CAC TGA CAA AAC GCA GAA CT
	Vt_2Probe	FAM-ACT-GAA CTC CAT TAA CGC CAG ATA TGA-TAMRA
Conventional PCR *stx*$_1$ WHO Collaborating Centre for Reference and Research on *Escherichia* and *Klebsiella* (132)	vtx1-det-F1	GTA CGG GGA TGC AGA TAA ATC GC
	vtx1-det-R1	AGC AGT CAT TAC ATA AGA ACG YCC ACT
Conventional PCR *stx*$_2$ WHO Collaborating Centre for Reference and Research on *Escherichia* and *Klebsiella* (132)	F4	GGC ACT GTC TGA AAC TGC TCC TGT
	R1	ATT AAA CTG CAC TTC AGC AAA TCC
	F4-f	CGC TGT CTG AGG CAT CTC CGC T
	R1-e/f	TAA ACT TCA CCT GGG CAA AGC C

All primer sequences were checked against the original papers to ensure no transcription errors were made (120, 131, 132). Primers were centrifuged and reconstituted in 100 µL of Gibco Ultra Pure water (Life Technologies, Burlington, Ontario, Canada) and then prepared as 200 µL of 20 pmol/L stock solutions for use in the LAMP assay. See the appendix for a sample primer calculation.

3.4 Optimization

Each primer set was optimized by varying the concentrations of magnesium, *Bst* polymerase enzyme (New England Biolabs, Pickering, Ontario, Canada), temperature and amplification time in a 25 µL reaction volume. Concentrations of primers (1.6 µM FIP/BIP, 0.2 µM F3/B3, and 0.8 µM LF/LB), 0.2 mM dNTPs (Life Technologies, Burlington, Ontario, Canada) and 1 M betaine (Sigma-Aldrich, St. Louis, MO, USA) were kept constant. Each primer set was initially tested with $MgSO_4$ (Sigma-Aldrich, St. Louis, MO, USA) at the concentrations of 4, 6, 8 and 9 mM, respectively, as shown by Tables 3-2 and 3-3 using standardized conditions of temperature (65°C) and time (60 min). The Applied Biosystems GeneAmp PCR System 2700 was used for all LAMP reactions (Life Technologies, Burlington, Ontario, Canada) with the exception of the temperature optimization step, which utilized the Eppendorf Mastercycler EP (Mississauga, Ontario, Canada) gradient thermocycler.

Table 3-2: Reaction conditions for the optimization of $MgSO_4$ for the *stx*$_1$ primer set in a 25 µL reaction volume. Note that the *stx*$_1$ primer set lacks the LB primer.

Reagent	4 mM $MgSO_4$ (µL)	6 mM $MgSO_4$ (µL)	8 mM $MgSO_4$ (µL)	9 mM $MgSO_4$ (µL)
5 M Betaine	5	5	5	5
30 mM $MgSO_4$	3.33	5	6.67	7.5
Bst Buffer	2.5	2.5	2.5	2.5
2.5 mM dNTPs	2	2	2	2
Water	5.54	3.87	2.2	1.37
FIP	2	2	2	2
BIP	2	2	2	2
F3	0.25	0.25	0.25	0.25
B3	0.25	0.25	0.25	0.25
LF	1	1	1	1
16U *Bst* polymerase	0.13	0.13	.0.13	0.13
Template DNA	1	1	1	1

Table 3-3: Reaction conditions for the optimization of $MgSO_4$ for the *stx*$_2$ primer set in a 25 µL reaction volume.

Reagent	4 mM $MgSO_4$ (µL)	6 mM $MgSO_4$ (µL)	8 mM $MgSO_4$ (µL)	9 mM $MgSO_4$ (µL)
5 M Betaine	5	5	5	5
30 mM $MgSO_4$	3.33	5	6.67	7.5
Bst Buffer	2.5	2.5	2.5	2.5
2.5 mM dNTPs	2	2	2	2
Water	4.67	3	1.33	0.5
FIP	2	2	2	2
BIP	2	2	2	2
F3	0.25	0.25	0.25	0.25
B3	0.25	0.25	0.25	0.25
LF	1	1	1	1
LB	1	1	1	1
16 U *Bst* polymerase	0.13	0.13	.0.13	0.13
Template DNA	1	1	1	1

The optimal $MgSO_4$ concentration was then tested with 8, 12, and 16 U of *Bst* Polymerase. The chosen $MgSO_4$ and *Bst* polymerase concentrations were tested for DNA extracted from cell suspensions containing 10^7,10^6 and 10^5 CFU (colony forming units) of the Sakai strain (refer to 2.2.5) at amplification times of 30, 60, 90 and 120 minutes respectively to determine the minimum time required for the amplification. The chosen concentrations of $MgSO_4$, *Bst* polymerase, and time were then tested with Sakai DNA extracted from the 10^7 CFU cell suspension using temperatures ranging from 60°C to 70°C on an Eppendorf

Mastercycler EP gradient thermocycler (Eppendorf AG, Hamburg, Germany) to determine the optimal amplification temperature.

3.5 Enumeration of 0.5 OD Bacterial Suspensions in terms of CFU/mL

Bacterial suspensions were prepared in saline to an optical density of 0.5 OD using the DADE Micrometer spectrophotometer (Dade Behring, Deerfield, Illinois, USA) and serially diluted 1/10 from 10^{-1} to 10^{-5}. Ten microlitres of each dilution was plated out on sheep blood agar plates (BAPs) and incubated 18-24 hours at 37°C as shown in Figure 3-2. Following incubation, colonies were counted on plates where the dilutions produced a countable amount of colonies and the CFU/mL present in each dilution determined.

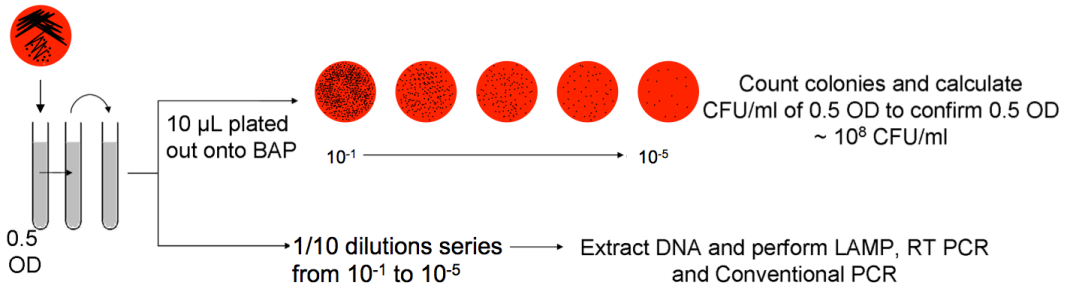

Figure 3-2: Schematic of the determination of sensitivity of LAMP, RT PCR and conventional PCR (bottom) and enumeration of 0.5 OD in terms of CFU/mL.

3.6 Determination of Sensitivity

The sensitivity of LAMP, RT-PCR and conventional PCR was determined using the positive control Sakai strain. A 10^{8} CFU/mL cell suspension of the Sakai strain cell suspension was serially diluted 1/10 from 10^{-1} to 10^{-5} and the cell concentration (CFU/ml) was confirmed as in 3.5. DNA was extracted from an aliquot of 200 µL of each concentration using the MagaZorb™ protocol on the KingFisher extractor. See appendix for sensitivity calculations. A 1 µL volume of DNA was used as the template in each amplification reaction and 10 µL of each of cell suspension from 10^{-3} to 10^{-7} were plated on BAP to determine the colony

forming units (CFU)/mL. Each assay was performed in replicates of 4 to show reproducibility of the assay.

3.7 Determination of Specificity

To determine the specificity of the assays, a panel consisting of the following bacteria were included: *Staphylococcus aureus (*ATCC 25923*), Staphylococcus epidermidis (*ATCC 29887*), Enterococcus faecalis (*ATCC 29212*), Micrococcus luteus (*ATCC 49732*), Staphylococcus saprophyticus (*ATCC 15305*), Proteus mirabilis (*ATCC 43071*), Yersinia enterocolitica (*ATCC 9610*), Salmonella typhimurium (*ATCC 14028*), Serratia marcescens (*ATCC 8100*), Shigella sonnei (*clinical isolate A79*), Shigella flexneri (*ATCC 12022*), Klebsiella pneumoniae (*ATCC 13883*), Proteus vulgaris (*ATCC 13315*), Pseudomonas aeruginosa (*ATCC 27853*), Enterobacter cloaecae (*ATCC 13047), *E.coli* O55:B5 (clinical isolate A301), *E.coli* O86:B7 (clinical isolate A303), *E.coli* O128:B12 (clinical isolate A305), *E.coli* O111:B4 (clinical isolate A300), *E.coli* O121:B8 (clinical isolate A301), and *E.coli* (ATCC 25922). *E.coli* O157 (Sakai strain) was included as a positive control. All bacteria were cultured on BAP plates and incubated 18-24 hrs aerobically at 37°C. The extractions of DNA and amplification assays were carried out as described above.

3.8 Conventional PCR

Conventional PCR was performed using the protocol from the WHO Collaborating Centre for Reference and Research on *Escherichia* and *Klebsiella* (132). The reaction was carried out in a 25 µL reaction volume containing 1 µL purified bacterial DNA, 0.25 uM of each primer, 2.5 µL of 10 x buffer, 0.16 mM dNTPS (Life Technologies, Burlington, Ontario, Canada) and 1 unit of HotStar Taq (Qiagen, Valencia, California, USA). The remainder of the volume was made up with Gibco Ultra Pure water (Life Technologies, Burlington, Ontario, Canada). The thermal cycling protocol used was as follows: 95°C for 15 minutes, 35 cycles of 94°C for 30 seconds, 64°C for 30 seconds and 72°C for 30 seconds followed by 7 minutes at 72°C. The Applied Biosystems GeneAmp PCR System 2700 was used for all conventional PCR reactions (Life Technologies, Burlington, Ontario,

Canada). In each run, a positive DNA control extracted from a 10^8 CFU/mL suspension of *E.coli* O157:H7 Sakai cells, and a negative control of Gibco Ultra Pure water was included.

3.9 Real-time PCR (RT-PCR) Protocol

RT-PCR was performed using the ABI Prism® 7500 FAST light cycler (Applied Biosystems, Foster City, California USA). The assay was performed in a 25 µL reaction volume using 1 µL of purified DNA from bacteria isolates, 12.5 µL Taqman® Fast Universal Mix 2x no Amperase UNG (Life Technologies, Burlington, Ontario, Canada), 50mM VT Primer/Probe mix. The thermal cycling protocol used was at 95°C for 10 minutes, 40 cycles of 95°C for 3 seconds and 60°C for 30 seconds (131). Both positive and negative controls as described in 2.2.8 were included.

3.10 Detection of Amplified Products

Amplified products (10 µL) from the LAMP and conventional PCR assays were analyzed using 1.5% Invitrogen UltraPure agarose (Life Technologies, Burlington, Ontario, Canada) gels containing 70 pg/mL Ethidium Bromide. Electrophoresis was carried out at 155 volts for 1.0 hour in a 0.5x TBE running buffer (Fisher Scientific, Ottawa, Ontario, Canada) containing 0.045 M Tris-HCl, 0.045 M borate, 1mM EDTA and 0.1 µg/mL ethidium bromide. A 100 base pair DNA ladder (ThermoScientific, Rockford, Illinois, USA) was included in each run. RT PCR products were visualized as an amplification curve of ΔRn (background corrected normalized reporter value) vs. cycle number and samples were considered positive if a curve above the baseline of 0.2 was obtained.

3.11 Clinical Sample Selection

Clinical stool samples (n=819) were submitted to ProvLab from Lethbridge Regional Hospital, Lethbridge, Alberta, Canada from July 2011 to November 2011. A subset of 155 $stx_{1+/2+}$, stx_{1+2-}, stx_{1-2+}, *and* stx_{1-2-} samples were included as a blinded panel for testing with the optimized LAMP assay.

3.12 Enrichment of STEC in stool samples and crude DNA extraction

Clinical stool samples were enriched in 3 mL of MacConkey broth by adding 200 µL of stool to the broth and incubating at 37°C overnight. Following incubation, 200 µL of enriched culture from the middle of the broth was retrieved and placed into to a 1.5 mL microcentrifuge tube and centrifuged for 3 minutes at 13,000 x g. Following centrifugation, the supernatant was removed and the pellet was resuspended in 1 mL of 12 mM Tris buffer, pH 7.4. The suspension was centrifuged for 3 minutes at 13,000 x g and the supernatant was removed. The pellet was re-suspended in 200 µL of rapid lysis buffer (100 mM NaCl, 10 mM Tris-HCl [pH 8.3], 1 mM EDTA [pH9], 1% Triton X-100) and boiled for 15 minutes in a water bath (133). After boiling, the lysate was centrifuged for 15 min at 13 000 x g and the supernatant was removed, and diluted 1:10 in water for use as template in the LAMP assay.

3.13 LAMP Assay using crude DNA

The LAMP assay was performed as in Chapter 2, with the exception that 3 µL of crude DNA was used as template with a concordant decrease in water volume.

3.14 RT-PCR Assay using crude DNA

RT-PCR, the current gold standard for STEC detection, was performed as in Chapter 2 using 5 µL of crude DNA template. Results were taken from a previous project where 5 µL of template was used, rather than the 3 µL used in the LAMP assay. Only 3 µL of template was used in the LAMP reaction due to only being able to decrease the water volume of the reaction by the same amount.

3.15 Calculation of Sensitivity, Specificity, Positive Predictive Value and Negative Predictive Value

Sensitivity, specificity, positive predictive value and negative predictive value were calculated as follows:

$$\text{Sensitivity} = \frac{\text{True Positives}}{\text{True Positives} + \text{False Negatives}}$$

$$\text{Specificity} = \frac{\text{True Negatives}}{\text{True Negatives} + \text{False Positives}}$$

$$\text{Positive Predictive Value} = \frac{\text{True Positives}}{\text{True Positives} + \text{False Positives}}$$

$$\text{Negative Predictive Value} = \frac{\text{True Negatives}}{\text{True Negatives} + \text{False Negatives}}$$

3.16 Clinical Sample Selection For Sybr Green I Detection Study

Clinical stool samples (n=819) were submitted to ProvLab from Lethbridge Regional Hospital, Lethbridge, Alberta, Canada from July 2011 to November 2011. A blind panel of 70 *$stx_{1+/2+}$*, *stx_{1+2-}*, *stx_{1-2+}, and stx_{1-2-}* samples was prepared testing with the LAMP assay using a Sybr Green I (SG1) detection method.

3.17 Visual Detection with Sybr Green I and Optimization with LAMP

Working solutions of 5000x, 2500x, 1000x, 500x and 100x Sybr Green 1 were prepared from a stock solution of 10000x Sybr Green I (Lumiprobe, Hallandale Beach, Florida, USA) using sterile Gibco Ultra Pure water. One microlitre of each dilution was added post amplification to LAMP reactions run with DNA extracted from a $1.5x10^7$ CFU/mL suspension of the Sakai strain and visualized both with the naked eye and under ultraviolet (UV) light. Once a SG1 dilution was chosen for further testing, based upon the quality of visual results it produced, it was further tested in duplicate with a Sakai strain dilution series (10^8

CFU/mL cell suspension serially diluted 1/10 from 10^{-1} to 10^{-5}), in which SG1 was added either pre-amplification or post-amplification.

3.18 LAMP using the Sybr Green I Detection Method for Identifying *stx*$_1$ and *stx*$_2$ in Clinical Samples

The LAMP assay was performed using 3 µL of DNA extracted from clinical stool samples by the rapid lysis method and products visualized by the naked eye and ultraviolet light after the addition of 1 µL of 1000x SG1.

3.19 Sample Selection for Optigene Study

Clinical stool samples (n=819) were submitted to the ProvLab from Lethbridge Regional Hospital, Lethbridge, Alberta, Canada from July 2011 to November 2011. A blind panel of 70 *stx*$_{1+/2+}$, *stx*$_{1+2-}$, *stx*$_{1-2+}$, *and stx*$_{1-2-}$ samples was prepared for testing with the Genie II as in 3.12.

3.20 Use of the Genie II for Identifying LAMP Amplified *stx*$_1$ and *stx*$_2$ in Clinical Samples

LAMP reactions were set up as shown in Table 3-4. The LAMP primers used were the same as those used in previous stages of this study. Template DNA (3 µL) extracted from clinical samples enriched in MacConkey broth and incubated overnight was used, as with the previously developed LAMP reaction to aid in comparison between the two. The volume of reagents required to prepare the reaction mix was calculated based on the number of samples to be tested and the reaction mix was prepared. Aliquots containing 22 µL of reaction mix were pipetted into wells of the Genie Strips and template DNA was then added to the corresponding wells in the Genie Strips. Each run included a positive DNA control and negative water control. The strips were then centrifuged briefly in a microfuge and loaded onto the Genie II. The sample names were inputted into the machine and the reaction started using the preprogrammed STEC program.

Table 3-4: Contents of Optigene Genie II LAMP reaction per sample.

	***stx*$_1$**	***stx*$_2$**
Reagent	**Volume (µL)**	
Optigene Isothermal Mastermix	15	15
20 µM FIP	2	2
20 µM BIP	2	2
20 µM F3	0.25	0.25
20 µM B3	0.25	0.25
20 µM LF	1	1
20 µM LB	--	1
Water	1.5	0.5
Template DNA	3	3
Total Volume	25	25

Chapter 4: Results

4.1 LAMP Optimization

The optimal concentration of $MgSO_4$ for the *stx*$_1$ primer set is 6 mM (Figure 4-1). The gel images (Figure 4-1) show that 6 mM $MgSO_4$ is the optimal condition, giving a positive result at a cell concentration of 10^4 CFU/mL as compared to 4 mM and 8 mM detecting 10^7 CFU/mL and 10^6 CFU/mL respectively. Results for the 9 mM were not reproducible, as this concentration tended to not amplify the template DNA in lanes in the middle of the optimization series (See Figure 4-1).

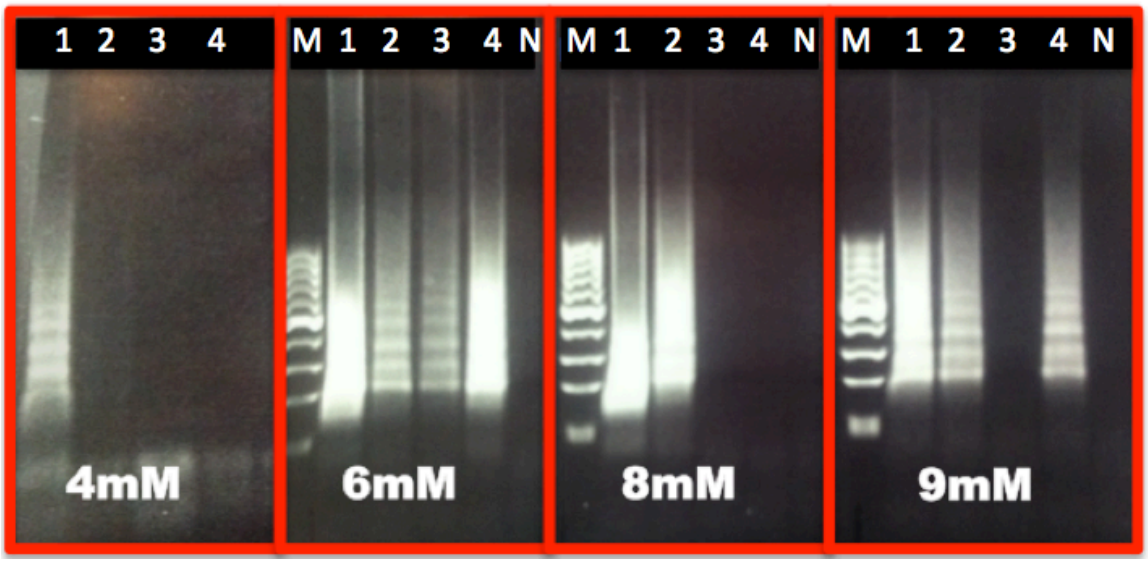

Figure 4-1: Results of $MgSO_4$ optimization for *stx*$_1$. From left to right each optimization set contains a DNA ladder (M) (with the exception of the 4 mM set), template DNA extracted from samples of 10^7, 10^6, 10^5, and 10^4 CFU/mL as shown in lanes 1-4, and a negative control (N) (with the exception of the 4 mM set).

The optimal concentration of $MgSO_4$ for the *stx*$_2$ primer set is 4 mM (Figure 4-2). The gel images show the 4mM $MgSO_4$ optimization set has the highest sensitivity with a detection level of 10^5 CFU/mL, while 6, 8 and 9 mM each have a sensitivity of only 10^6 CFU/mL.

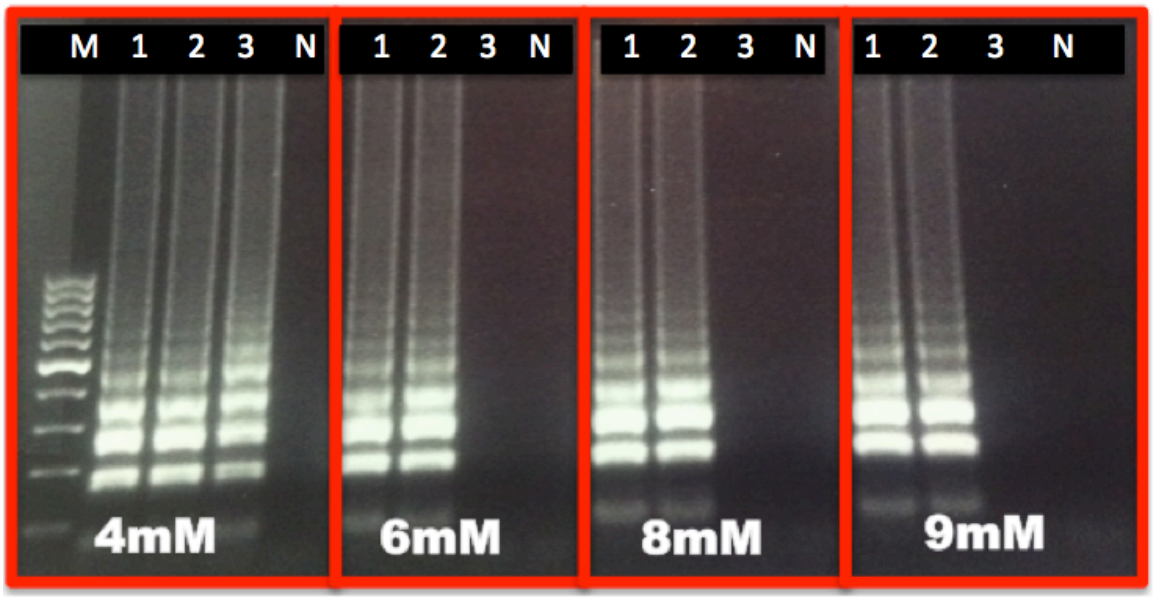

Figure 4-2: Results of $MgSO_4$ optimization for *stx*$_2$. The far left lane in the 4 mM set contains a DNA ladder (M). From left to right each optimization set contains template DNA extracted from samples of 10^7, 10^6, and 10^5 CFU/mL as shown in lanes 1-3, and a negative control (N).

The optimal *Bst* polymerase enzyme concentration for *stx*$_1$ is 12 U and 8U for *stx*$_2$ (Figures 4-3 and 4-4). *Stx*$_1$ showed similar results for 8 and 12 U, however 12 U had slightly clearer bands than 8 U and false positives were consistently seen with 16 U, as shown by bands in the negative control lane in the 16 U set. The best sensitivity for *stx*$_2$ was observed with 8U of *Bst* polymerase in the LAMP assay as bands appeared in the 10^5 CFU/mL lane, and only to the 10^6 CFU/mL lanes for 12 and 16 U.

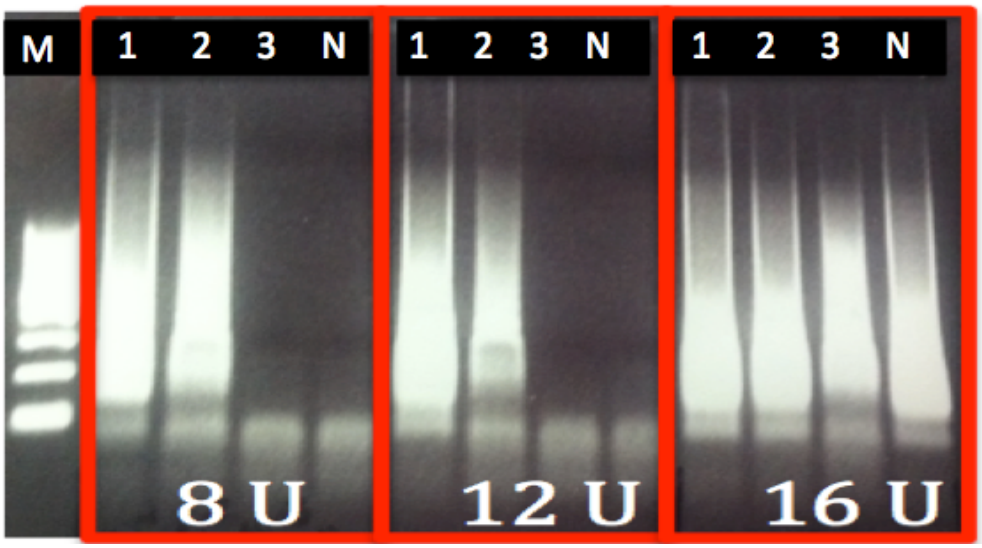

Figure 4-3: Results of *Bst* polymerase enzyme optimization for *stx*$_1$ using 6mM $MgSO_4$. The far left lane contains the DNA ladder (M), followed by the enzyme optimization sets of 8, 12 and 16 units of *Bst* polymerase. Each enzyme optimization set contains template DNA extracted from samples of 10^7,10^6, and 10^5 CFU/mL (lanes 1-3), and a negative control (N).

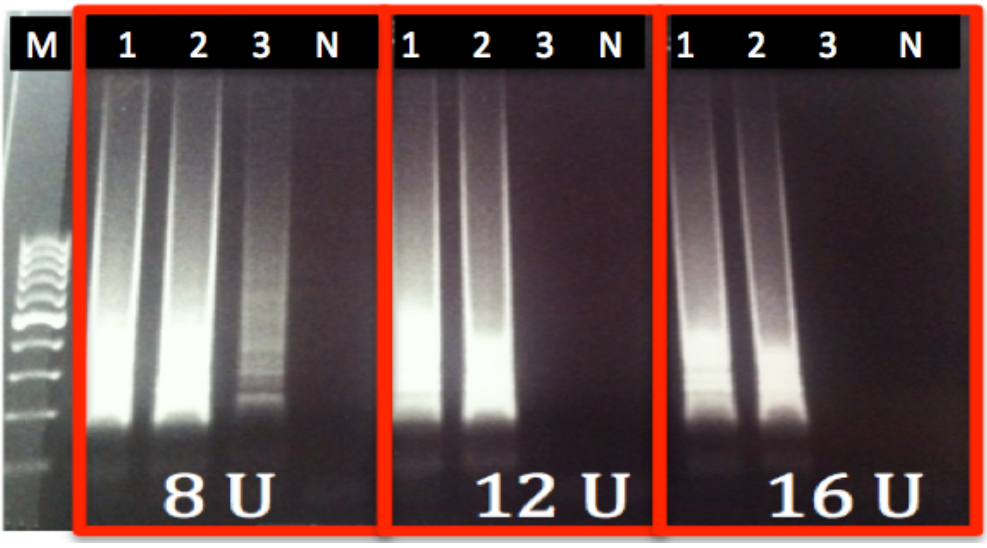

Figure 4-4: Results of *Bst* polymerase enzyme optimization for *stx*$_2$ using 4 mM $MgSO_4$. The far left lane contains the DNA ladder (M), followed by the enzyme optimization sets of 8, 12 and 16 units of *Bst* polymerase. Each enzyme optimization set contains template DNA extracted from samples of 10^7,10^6, and 10^5 CFU/mL (lanes 1-3), and a negative control.

The reaction time optimization (Figures 4-5 and 4-6 showed a run time of 90 minutes to be ideal for *stx*$_1$ and 60 minutes for *stx*$_2$. Neither primer set yielded results with a 30 minute run time.

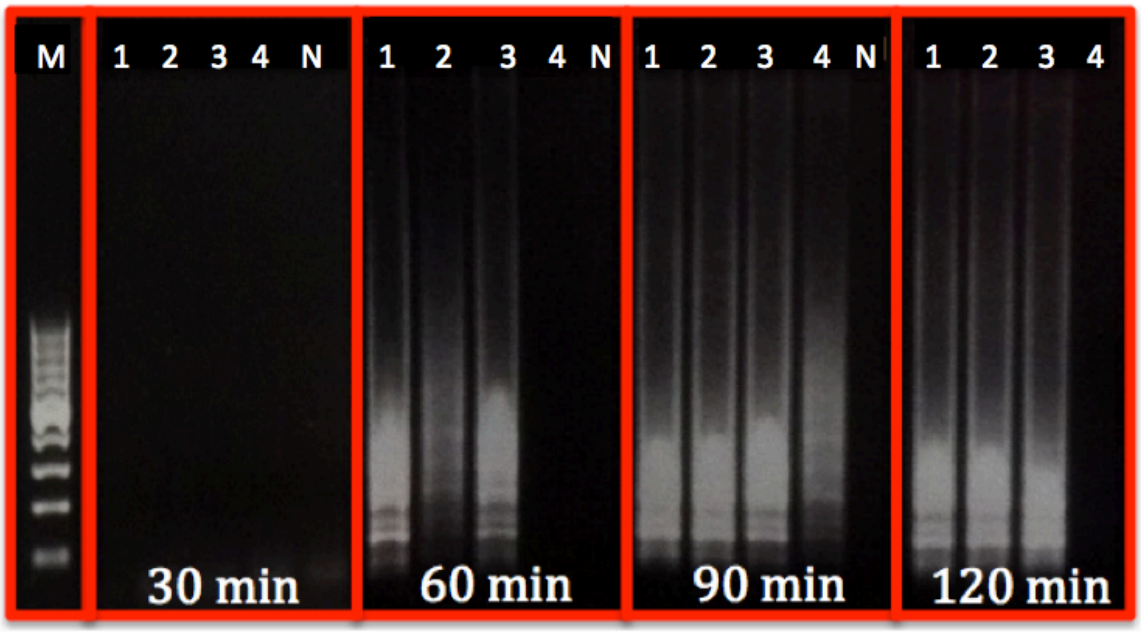

Figure 4-5 : Reaction time optimization for *stx*$_1$. The far left lane contains a DNA ladder (M). Each time set from left to right was run with template DNA extracted from samples of 10^7, 10^6, 10^5, and 10^4 CFU/mL (lanes 1-4), as well as a negative control (N) at 65°C (negative control not shown with 120 min set).

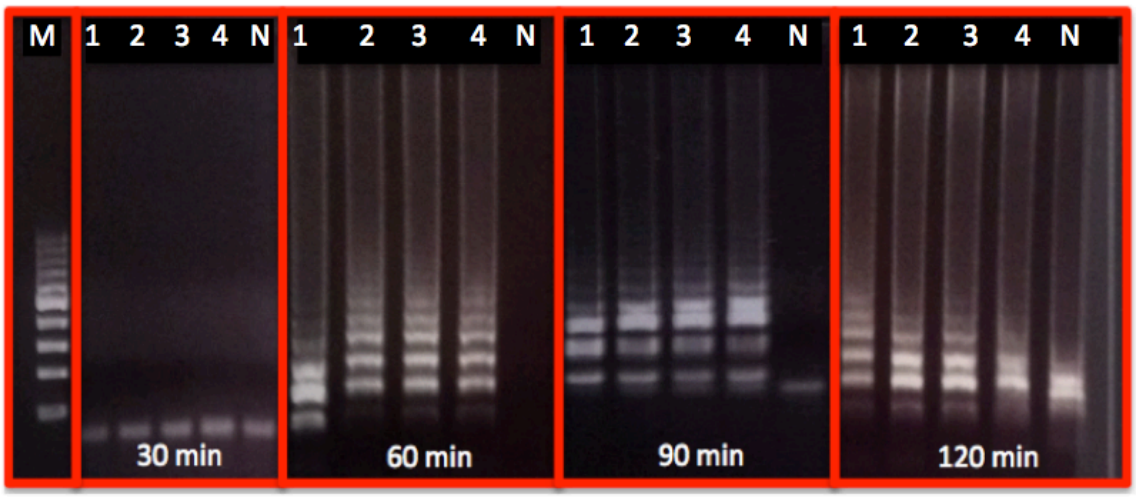

Figure 4-6: Reaction time optimization for *stx*$_2$. The far left lane contains a DNA ladder (M). Each time set from left to right was run with template DNA extracted from samples of 10^7, 10^6, 10^5, and 10^4 CFU/mL (lanes 1-4), as well as a negative control (N) at 65°C.

Following reaction time optimization the optimal reaction temperature was determined using an Eppendorf Mastercycler EP gradient thermocycler (Eppendorf AG, Hamburg, Germany). Optimal reaction temperatures were considered to be those that produced consistent results and were not near the temperature endpoint (where template no longer amplified). As shown below in Figures 4-7 and 4-8 the optimal reaction temperature for the *stx*$_1$ reaction was 65°C, while for *stx*$_2$ it was 64°C. False positive results in the negative control wells for *stx*$_1$ were consistently seen at 64°C and the same was seen with *stx*$_2$ for 60.7°C. The optimal temperature based on these results for both primer sets, was chosen to be 65°C, as this temperature produced consistent results and was lower than the temperature (approximately 67°C) where template failed to amplify.

Following optimization, the ideal reaction conditions for *stx*$_1$ were 6 mM $MgS0_4$, 12 U *Bst* polymerase, 65°C reaction temperature and a reaction time of 90 min (Table 4-1). The ideal reaction conditions for *stx*$_2$ were 4 mM $MgS0_4$, 8 U *bst* polymerase, 65°C reaction temperature and a reaction time of 60 min (Table 4-1).

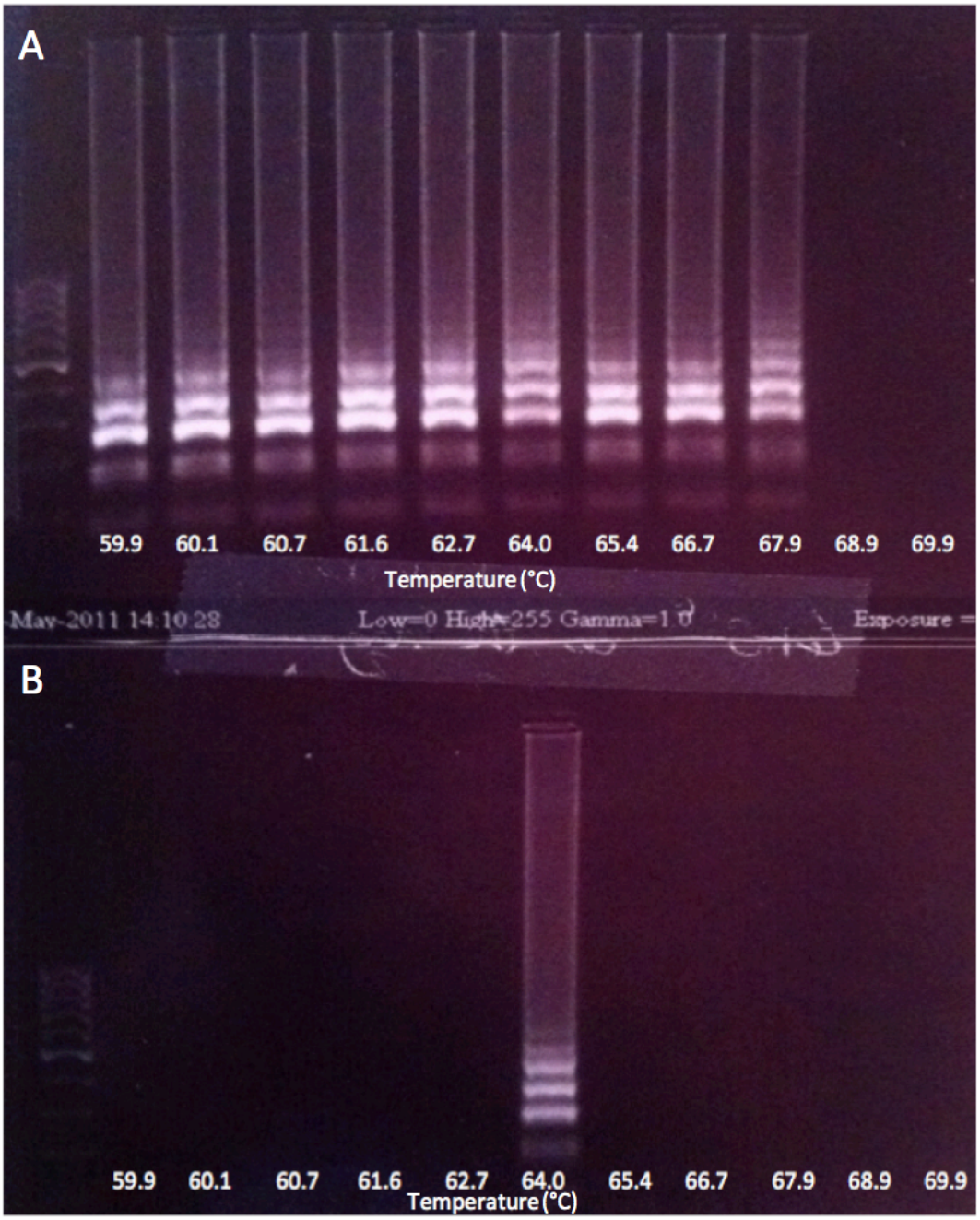

Figure 4-7: (A) Temperature optimization of *stx*$_1$ using a 10^7 CFU/mL dilution of the Sakai strain as DNA template and reaction conditions of 6mM $MgSO_4$, 12 U *Bst* polymerase, and a 60-minute run time. (B) Corresponding negative water controls for each temperature. In both (A) and (B) the far left lane contains a DNA ladder.

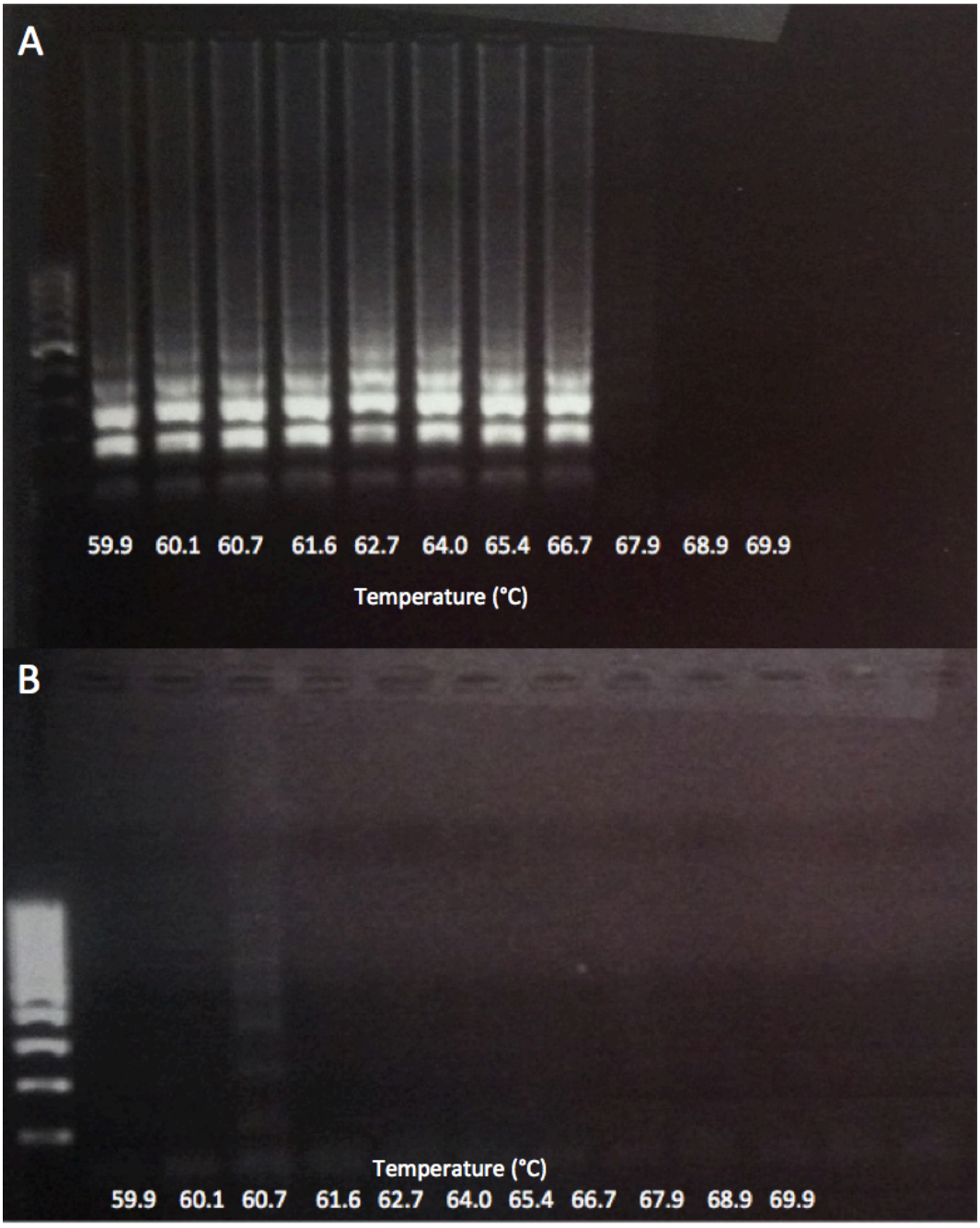

Figure 4-8: (A) Temperature optimization of *stx*$_2$ using a 10^7 CFU/mL dilution of the Sakai strain as DNA template and reaction conditions of 4 mM $MgSO_4$, 12 U *Bst* polymerase, and a 60 minute run time. (B) Corresponding negative water controls for each temperature. In both (A) and (B) the far left lane contains a DNA ladder.

Table 4-1: Summary of the optimized LAMP reaction conditions for *stx*$_1$ and *stx*$_2$.

	***stx*$_1$**	***stx*$_2$**
[$MgSO_4$]	6mM	4mM
Enzyme	12 U	8 U
Temperature	65°C	65°C
Time	90 min	60 min

4.2 Enumeration of 0.5 OD Bacterial Suspensions in terms of CFU/mL

Following overnight incubation, the BAP plates were examined and colonies counted. The plates onto which the 10^{-1} to 10^{-3} dilutions were plated had too many colonies to count, while the 10^{-4} plate, done in duplicate, had 45 and 48 colonies respectively giving an average of 47 colonies. Therefore, the concentration of the 0.5 OD cell suspension contained 4.7 x 10^7 CFU/ml or 0.5 x 10^8 CFU/mL. The results of this experiment were confirmed upon repeat. Calculations were performed as follows:

Calculation of CFU/mL in 0.5 OD Cell Suspension:

$$\frac{47}{0.01\text{mL}} = \frac{x}{1\text{mL}} = 4700 \text{ CFU/mL}$$

In the 10^{-4} dilution 4700 CFU/mL were present, therefore the original undiluted 0.5 OD specimen contained 4.7 x 10^7 CFU/mL or 0.5 x 10^8 CFU/mL.

4.3 Sensitivity of Amplification Assays

Initially sensitivity testing was unsuccessful due to inconsistent results using DNA as a template from the Sakai strain dilution series of cells for the LAMP assay without a heat denaturation step. Once a heat denaturation step (95°C for 15 min) was included pre-amplification, consistent end point detection results were obtained. Sensitivity testing, performed in quadruplicate using the Sakai strain (Table 4-2), yielded consistently positive results for the *stx*$_1$ primer set to between the 10^5 and 10^4 CFU/mL dilutions consistently, which corresponds to an average of 10 CFU per reaction. For *stx*$_2$ the reaction consistently remained positive to the 10^3 and 10^2 CFU/mL dilutions corresponding to 1 CFU.

Sensitivity testing with RT PCR showed the sensitivity for *stx*$_1$ to be 1 CFU and *stx*$_2$ to be 10 CFU, while for conventional PCR both primer sets had sensitivities of 1 CFU.

Table 4-2: Representations of sensitivity testing of LAMP, conventional PCR and real-time PCR using the Sakai strain (performed in quadruplicate).

CFU/mL Detected by *stx*$_1$ Primer Set					
	10^6	10^5	10^4	10^3	10^2
LAMP	+	+	+	-	-
Conventional PCR	+	+	+	+	+
RT-PCR	+	+	+	+	+
CFU/mL Detected by *stx*$_2$ Primer Set					
	10^6	10^5	10^4	10^3	10^2
LAMP	+	+	+	+	+
Conventional PCR	+	+	+	+	+
RT-PCR	+	+	+	-	-

Sensitivity testing was repeated with another strain of *stx*$_{1/2}$ positive *E. coli,* VT483, and all assays were found to be more sensitive with this strain. LAMP and conventional PCR were both sensitive to 1 CFU for *stx*$_1$ and *stx*$_2$ while RT PCR had a sensitivity of 1 CFU for *stx*$_1$ and 10 CFU for *stx*$_2$ (data not shown).

4.4 Specificity of Amplification Assays

When tested against the specificity panel using the LAMP assay described in 3.7, the *stx*$_1$ primer set produced false positives for *Salmonella typhi* and *Shigella sonnei*. False positives with the *stx*$_2$ primer set were seen for *Enterococcus faecalis*, *E. coli* ATCC 25922 and *Shigella dysenteriae*. All discrepancies were resolved upon repeat. Based upon these results the specificity of the primer sets were 90% for *stx*$_1$ and 86% for *stx*$_2$. Both RT PCR and conventional PCR had specificities of 100% for both primer sets.

4.5 Cost analysis and Assay Comparison

When using DNA extracted using the KingFisher the total cost per 10 *stx*$_1$ and *stx*$_2$ reactions, not including controls or technologist time, is approximately $90 for LAMP and $100 for conventional PCR including the cost of agarose gel. The cost of 10 *stx*$_1$ and *stx*$_2$ reactions using RT PCR is approximately $100. If using a rapid lysis DNA extraction LAMP costs approximately $45 while conventional PCR (including agarose gel) costs approximately $60 per 10 reaction sets. RT PCR using a rapid lysis extraction costs $56 per 10 reaction sets.

A comparison of the three methods, including turn around time, cost per test, equipment required, temperature, results, sensitivity and specificity is shown in Table 4-3.

Table 4-3: Comparison of LAMP, RT PCR and conventional PCR.

	LAMP	RT PCR	Conventional PCR
Turn Around Time	3 hrs	65 min	4 hrs
Cost / 10 Tests Using Rapid Lysis DNA Extraction	$45	$56	$60
Equipment	Heat Block	7500 Fast RT PCR System	ABI Geneamp PCR System 2700
Temperature	65°C	40 Cycles of 95 and 60°C	40 Cycles of 95,64, and 72°C
Results	Bands on gel	Amplification Curve	Bands on gel
Sensitivity (cfu)			
stx$_1$	1	1	1
stx$_2$	1	10	1
Specificity			
stx$_1$	90%	100%	100%
stx$_2$	86%	100%	100%

4.6 Blinded Panel of Clinical Samples

Agarose gel electrophoresis was used for the analysis of the LAMP amplified product. When compared to results obtained by RT-PCR (the current method used at the Provincial Laboratory in Alberta), there was 1 false negative result for *stx*$_1$, 7 false positives for *stx*$_1$ and 1 false positive for *stx*$_2$, all of which were resolved upon repeat analysis. The LAMP assay had a sensitivity of 90%, specificity of 95%, positive predictive value (PPV) of 56%, and negative predictive value (NPV) of 99% for *stx*$_1$ prior to repeating discrepant samples. For *stx*$_2$, prior to repeats, the LAMP assay was 100% sensitive, 99% specific and had a PPV of 89% and NPV of 100%. These results are summarized in Figure 4-9.

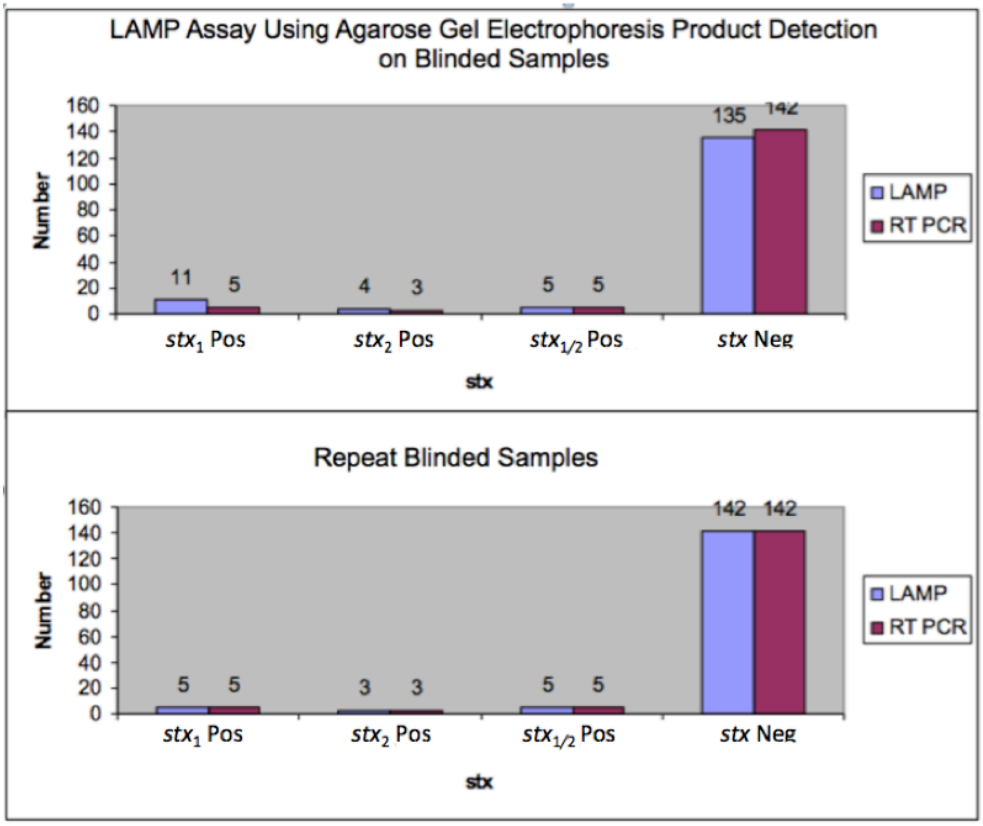

Figure 4-9: Results of the blinded panel of clinical samples run with LAMP using an agarose electrophoresis product detection method compared to RT-PCR results from a previous study.

4.7 Visual Detection of LAMP Products with Sybr Green

Initially, 1 µL of 1000x SG1 was added to *stx*$_1$ and *stx*$_2$ positive (Sakai strain dilution series) and negative LAMP reactions (water controls and *stx*$_{1/2}$ negative *E. coli* ATCC 25922) was used as a starting point to determine the characteristics of positive and negative results using the fluorescent dye. As shown in Figure 4-10, positive results are characterized by an 'apple green' color to the naked eye, and green fluorescence under UV light while negative results remain the orange color of the dye itself and fail to fluoresce when exposed to UV light.

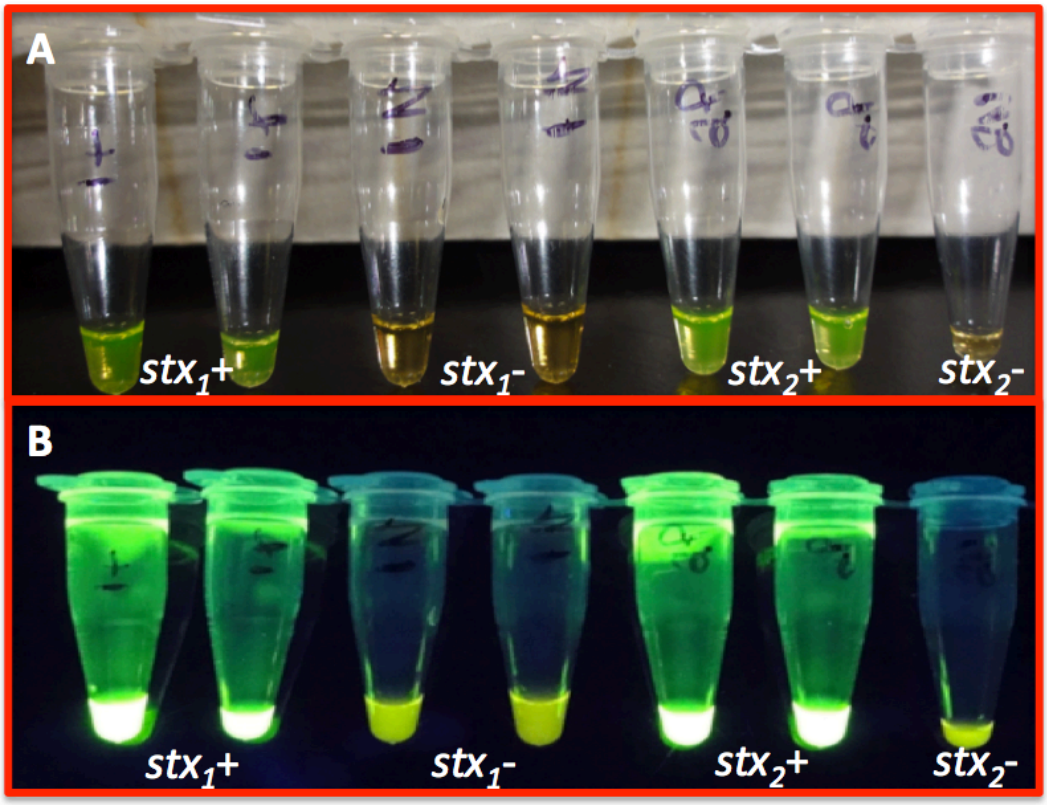

Figure 4-10: (A) *stx*$_1$ and *stx*$_2$ positive (green) and negative (orange) samples with 1 uL 1000x Sybr Green 1 added post-amplification and visualized using visible light. (B) *stx*$_1$ and *stx*$_2$ positive (green fluorescence) and negative (no fluorescence) samples with 1 uL 1000x Sybr Green 1 added post-amplification and visualized using ultraviolet light.

To determine the optimal concentration of SG1, 1 µL of 5000x, 2500x, 1000x, 500x, and 100x SG1 were added post-amplification to LAMP reactions run with 1 µL DNA extracted from a 1.5x10^7 CFU/mL suspension of Sakai strain as the target. The concentration of 5000x SG1 overwhelmed the reaction and

remained orange under visual light but did fluoresce under UV, while the 100x dilution was to weak to visualize with the naked eye, and fluoresced minimally under UV light. Concentrations of 500x, 1000x, and 500x SG1 all appeared green to the naked eye and fluoresced a bright green under UV light (Figure 4-11) .The 1000x SG1 concentration was chosen to move forward, in hopes that the 'middle-ground' concentration would have less chance of either overwhelming the amount of DNA in the reaction or failing to detect it.

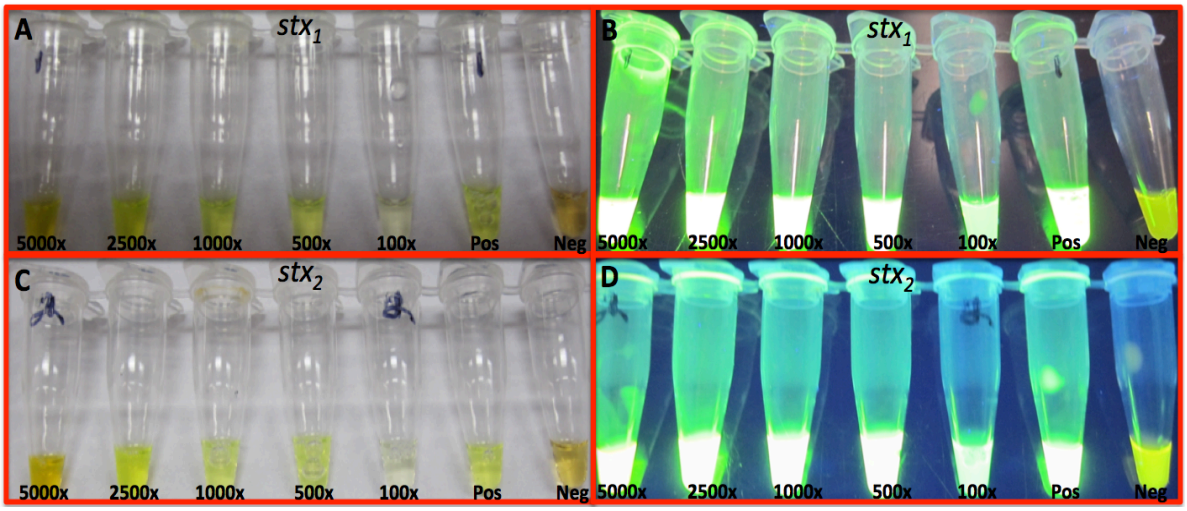

Figure 4-11: Sybr Green dilution series using 1 µL 5000x, 2500x, 1000x, 500x and 100x SG1. (A) *stx*$_1$ visualized with visible light. (B) *stx*$_1$ visualized with UV light. (C) *stx*$_2$ visualized with visible light (D) *stx*$_2$ visualized with UV light.

The addition of 1 µL SG1 post-amplification to the Sakai *E. coli* dilution series resulted in sensitivities of detection between 1 CFU and 10 CFU for both *stx*$_1$ and *stx*$_2$, which was further confirmed by running the LAMP products on an agarose gel (data not shown). The addition of 1 µL SG1 pre-amplification resulted in negative results for all dilutions in the series when detected by visible light, UV light and agarose gel electrophoresis (Figure 4-12).

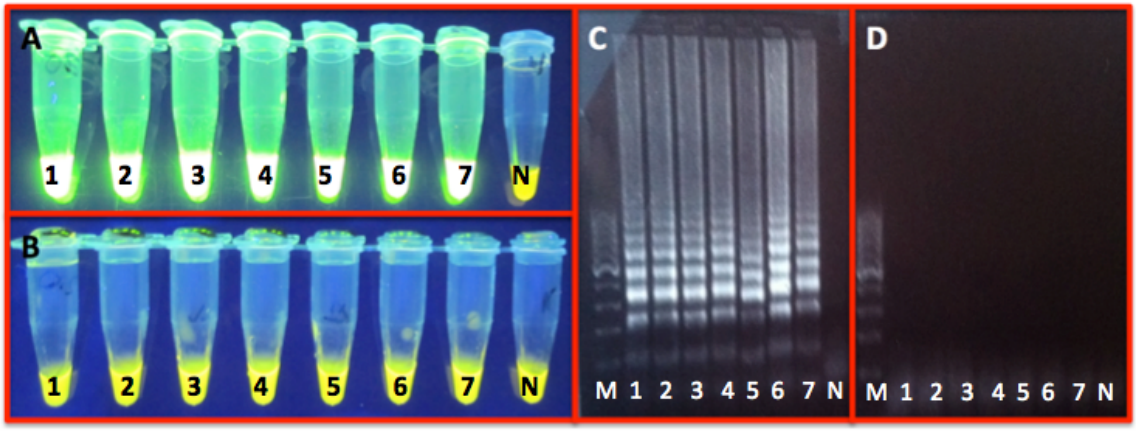

Figure 4-12: Dilution series of Sakai strain, each set contains template DNA extracted from samples of 10^8, 10^7, 10^6, 10^5, 10^4, 10^3 and 10^2 CFU/mL as represented by tubes 1-7 in A and B, and a negative control (N). The far left lane in agarose gels contain a DNA marker (M). (A) *stx*$_2$ with SG1 added post-amplification with UV light visualization (C) further confirmed by gel electrophoresis. (B) SG1 added pre-amplification with UV light visualization and (D) with agarose gel electrophoresis.

When SG1 visualized under UV light was used to detect amplified product for the LAMP assay using the blinded panel of clinical samples, 4 false positives were observed for *stx*$_1$ and 14 false positive results were observed for *stx*$_2$ (Figure 4-13). No false negatives were seen for either primer set. Based on this data, the calculated sensitivity was 100%, with a specificity of 93%, PPV of 76% and NPV of 100% for *stx*$_1$. For *stx*$_2$, this assay has a sensitivity of 100%, specificity of 77%, PPV of 39% and NPV of 100% were obtained. Samples were retested but 7% of the samples (n=70) remained discordant when compared with RT PCR.

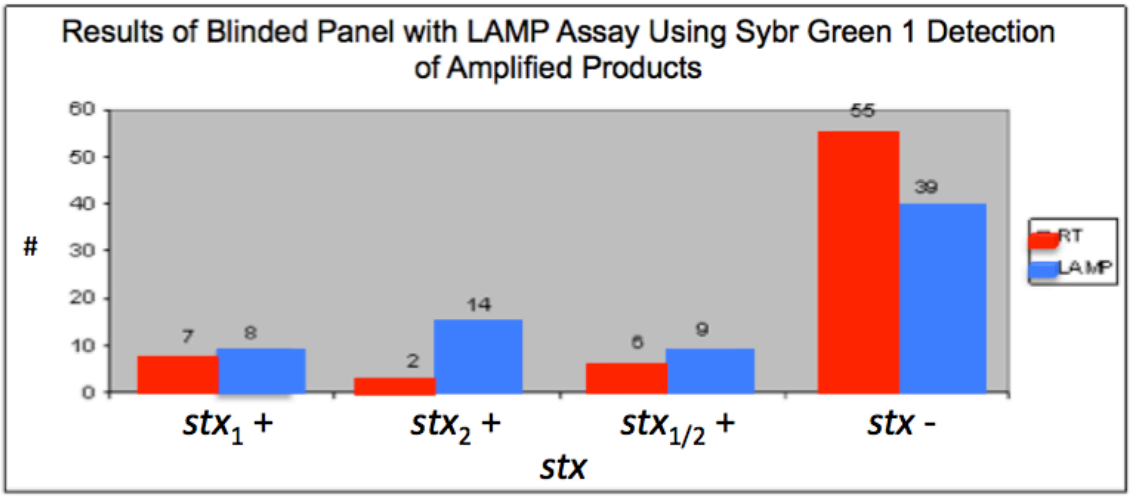

Figure 4-13: Results of the blinded panel of clinical samples run with LAMP using Sybr Green I product detection compared to RT-PCR results from a previous study.

4.8 Detection of LAMP Products Using the Optigene Genie II

For each positive sample, time to positivity and annealing temperature of the amplified product were recorded and the fluorescent data amplification and annealing peaks checked to ensure positive results were true positives. All 70 samples agreed with the results obtained previously by RT-PCR with the exception of one sample, which was positive for *stx*$_1$ with the Genie II and negative by RT-PCR. Upon repeat analysis the discrepant sample was negative, confirming it to be a false positive.

Chapter 5: Discussion

5.1 LAMP Optimization

The LAMP reaction was successfully optimized for both the *stx*$_1$ and *stx*$_2$ primer sets for $MgSO_4$ and enzyme concentration, reaction temperature and time. Initially, problems were encountered as artifact was frequently seen in developed gels and consistent results could not be obtained on repeat. Including a heat denaturation step proved necessary for repeatability and elimination of artifact. This is contrary to the report issued in 2001 by Nagamine *et al.*, who found that betaine sufficiently caused DNA strand separation through an unknown mechanism allowing for the elimination of the heat denaturation step (108). Some studies have successfully eliminated the heat denaturation step, while others such as that by Suzuki *et al.*, have found heat denaturation to be necessary for reproducibility or to improve reaction sensitivity (124, 134, 135). Elimination of the heat denaturation step can decrease sensitivity by as much as 200-fold (124). Likely, the need for heat denaturation depends on the DNA being tested and the reaction optimization process will show whether the step is necessary for the particular DNA and primer sets being used.

The reaction time chosen for both primer sets was 60 minutes despite the *stx*$_1$ primer set having slightly higher sensitivity at 90 minutes. Having equivalent reaction times for each primer set at 60 minutes decreases the overall turn around time of the reactions with a minimal decrease in sensitivity. The sensitivity of the *stx*$_1$ primer set was calculated to be 10 CFU while the sensitivity for *stx*$_2$ was 1 CFU using the Sakai strain of *E. coli*. When the *E. coli* VT483 dilution series was used both primer sets were able to detect the target at concentrations as low as 1 CFU. Therefore, both primer sets are able to detect small amounts of DNA using a reaction time of 60 minutes.

LAMP was shown to be very specific when tested against a panel of Gram positive and negative organisms; all false positives were resolved upon one repeat. These false positive results were likely due to aerosolization of amplicons resulting in cross contamination of opened tubes, a problem that has been

encountered in previous studies (115, 125). The high degree of specificity in the LAMP reaction has been attributed to the requirement for 6 primers to bind regions of the target DNA (102). The *stx*$_1$ primer set did produce positive results when tested with *Shigella dysenteriae* likely due to the similarity in toxin structure between the two organisms.

In this study, LAMP products were detected using agarose gel electrophoresis and ethidium bromide. Previous studies have shown that positive LAMP reactions produce a large amount of white magnesium pyrophosphate precipitate due to pyrophosphate ions combining with free magnesium ions in the buffer solution as the reaction is taking place, leading to positive results being visible to the naked eye (109, 110). The LAMP reaction tested in this study did not produce enough of this precipitate to allow visual detection of reaction products; therefore, visualization of products using electrophoresis was necessary. Other reports agree with the findings in this study and reported that turbidity can be difficult to detect using the naked eye making alternate methods of detection such as gel electrophoresis necessary (112, 126). A previous study has shown that production of visual precipitate can be primer set-dependent; with some primers sets producing visible magnesium pyrophosphate while others produce no visual precipitate at all (112).

Cost analysis of all three methodologies has shown that for 10 *stx*$_1$ and *stx*$_2$ reactions using a rapid lysis DNA extraction, conventional PCR is the most expensive ($60), followed by RT-PCR ($56) and LAMP ($45). The cost of the LAMP assay in its current state is attributed mainly to the agarose gel electrophoresis product detection step. The cost of LAMP is further decreased when one takes into account the equipment required to perform each assay, as LAMP does not require sophisticated equipment such as thermal cyclers or RT-PCR platforms.

LAMP has been shown to be a cost effective method of detecting the *stx*$_1$ and *stx*$_2$ genes of STEC that is both sensitive and specific. False positive results encountered with the optimized LAMP assay were likely due to the assay's high degree of sensitivity. The simple equipment required to perform the assay makes

it possible to perform in any laboratory setting. Eliminating the agarose gel detection method and replacing it with a visual detection method incorporating a fluorescent marker dye can further decrease cost. This chapter assessed LAMP detection of *stx* genes using purified DNA from bacterial culture. DNA extracted from clinical stool samples will be amplified with LAMP to assess the reliability of LAMP in clinical situations for the diagnosis of STEC infection without the isolation of pure culture from clinical specimens.

5.2 Assessment of the Ability of LAMP to Detect *stx* in Clinical Samples

LAMP performed comparably to RT-PCR when tested on clinical stool samples using DNA extracted by manual rapid lysis and analyzed by agarose gel electrophoresis. After testing with crude DNA from 155 stool samples LAMP, had comparable sensitivity, specificity, positive predictive value and negative predictive value to the current method used at the Provincial Laboratory in Edmonton, RT-PCR. However, due to the possibility of false positive results occurring, it is recommended at this time to perform repeat testing on all samples with positive results.

There are many advantages to the LAMP assay over the current RT-PCR method. Since LAMP does not require expensive equipment such as thermal-cyclers or RT-PCR platforms, it can be used in nearly any diagnostic laboratory. Assay set-up and interpretation of results is simple to perform and does not require intensive training.

In this study, LAMP was found to be comparable to RT-PCR. Most of the results that did not initially correlate were due to false positivity, likely caused by environmental contamination. This is an issue with the LAMP assay, as its high sensitivity makes it more susceptible to contamination. These findings are supported by other studies, which have shown LAMP to be comparable in sensitivity and specificity to RT-PCR (121-124, 136).

Although the LAMP method has many advantages over conventional and RT-PCR, it is not without limitations. During specificity testing and work with clinical samples, false negative and false positive results were obtained. False

positives occurred most often while false negatives were relatively rare, which supports previous findings that the LAMP assay is prone to environmental contamination. Upon repeat testing all false positive results became negative. Previous studies have encountered problems with false positive results, and were attributed to the large volumes of amplicons produced by the highly efficient reaction (111, 115, 124, 125). As such, any unnecessary reaction manipulation must be strictly avoided and ideally master mix and product detection done in completely separate areas (124). When setting up LAMP reactions, the area must be extremely clean and free of any post-amplification products.

The results obtained in this study demonstrate that LAMP is a viable alternative to the current methodology in our laboratory, RT-PCR, for testing *stx* status of clinical stool samples. Further study is required to eliminate the need for product detection by agarose gel electrophoresis, to decrease the turn-around-time and cost making it more attractive to laboratories with limited resources. In addition, further work needs to be completed to decrease the incidence of false positive results due to environmental contamination. LAMP is a valuable; cost effective method for detection of *stx* genes in clinical stool samples.

5.3 Visual Detection of LAMP Products with Sybr Green I

Sybr Green 1 shows promise as a method of detecting LAMP products without agarose gel electrophoresis, as both positive and negative reactions were successfully detected using both pure DNA and crude DNA extracts from clinical stool samples. The cost of LAMP using this product detection system and a rapid lysis DNA extraction is approximately $35 per 10 samples. As agarose gel electrophoresis takes approximately 1 hour and costs between another $6-10 for 10 samples, the potential savings in TAT and cost by using a SG detection system is significant.

In addition to saving time and cost, the SG1 detection system is simple to perform. A 1 µL volume of 1000x SG1 is added to the LAMP reaction post-amplification and observed under both visual light for orange (negative) to green (positive) color change and UV light for fluorescence (positive). These results

and previous studies have demonstrated that, SG1 must be added to the LAMP reaction post-amplification, as adding SG1 pre-amplification results in reaction inhibition (Figure 4-12) (125).

As SG1 cannot be added to the reaction pre-amplification, the LAMP reaction is not a closed-tube system and thus is vulnerable to contamination from amplicons in the environment. LAMP is a highly efficient reaction, generating a large amount of amplicons, which easily aerosolize when the caps are opened for SG1 addition (115, 125, 127). This leads to false positive results, and likely accounts for the poor reproducibility of results seen in this study when using the SG1 detection system with clinical samples. In order to mitigate the risk of contamination a closed-tube system such as that by developed by Tao *et al.,* is necessary (125). Tao *et al.,* encapsulated SG1 in a microcrystalline wax bead that does not melt at reaction temperatures preventing reaction inhibition (125). When the LAMP reaction is complete, the tubes are simply heated to the melting point of the wax bead allowing the SG1 to interact with the DNA produced in the reaction and the wax to provide another barrier between the environment and the reaction (125). Another option is to use a type of reader, which maintains the reaction as a closed system.

The SG1 detection method optimized in this study provides a simple, cost effective method of product detection for the LAMP assay. However, further study is required to eliminate the risk of false positives due to amplicons being aerosolized when tubes are opened for addition of the dye. If the LAMP assay is converted into a fully closed system, the occurrence of false positives should decrease dramatically resulting in improved assay performance, making it a viable option for detecting *stx*$_{1/2}$ in clinical settings.

5.4 Detection of LAMP Products Using the Optigene Genie II

The results from the Genie II correlated nearly perfectly to those obtained by RT PCR. The sensitivity of the LAMP assay using this instrument was 100% for both *stx*$_1$ and *stx*$_2$ while the specificity was 98% for *stx*$_1$ and 100% for *stx*$_2$. The positive predictive value was 92% for *stx*$_1$ and 100% for *stx*$_2$ while both *stx*$_1$

and *stx*$_2$ had a negative predictive value of 100%. No false negatives were obtained and only one false positive was observed which was resolved after 1 repeat. The Genie II LAMP method was also much faster than the manual LAMP method previously described in this study, with positive results consistently generated in under 20 minutes.

Compared to the LAMP method developed in this study, the Genie II was much less susceptible to false positive results. This is likely due to the fact that the Genie II assay is a completely closed system. Once the template DNA is added, the tubes are closed with no further manipulation, which prevents environmental contamination. This is a great advantage over the LAMP assay developed in this study where agarose gel electrophoresis or Sybr Green 1 are required for analysis. The same primers were used for both the manual LAMP method and the Genie II assay; therefore, the primers can be ruled out as a cause of inconsistent reactions with the manual method as the same primers produced reliable results with the Genie II. This provides additional evidence that the manual LAMP method is very susceptible to environmental contamination.

Further advantages of the Genie II system include the simplicity of setting up the reactions, as well as the ease of use of the instrument itself. Since the assay can be performed on the instrument using power from either electrical outlets or an internal rechargeable battery, the system is highly portable (129). The Genie II's simple touch screen interface allows for simple assay programming and reaction set-up. Operators are able to monitor the reaction as it occurs, as the Genie II monitors the fluorescence produced by the reaction in real time. Annealing curves can also be monitored in order to confirm the validity of positive results. For further optimization of reactions, running a temperature gradient is possible (129).

As the Genie II is a relatively new system, it is not without disadvantages and could benefit from further refinement. Currently, the system is only able accept two strip tubes (16 reactions) per run which limits the amount of reactions that can be performed in a day. At this time, the largest disadvantage of the Genie II LAMP system is the requirement of a computer for data transport from

the portable system and data print out. A further disadvantage is the overall cost of the system. The Genie II itself retails at nearly $20 000, and the user must use the strip tubes and isothermal mastermix provided by Optigene which further increases cost per test (129). The LAMP assay developed in this study has a cost of $45 per 10 reactions using rapid lysis DNA extraction and agarose gel electrophoresis product detection and requires no special equipment. The Genie II is therefore significantly more costly than a 'manual' LAMP method such as the one described in this study as the instrument itself costs $20 000.

The Genie II is a promising automated LAMP system that produces consistent and reliable results due to its advantage of being a closed tube system. With further refinement in computer connectivity, the Genie II will be a user-friendly instrument that could be implemented for use in clinical laboratories. The portability of the Genie II makes it ideal for use in various locations from rural laboratories to field-testing sites. Smaller laboratories may have difficulty justifying the cost of the instrument, and in these cases the manual LAMP method remains a viable alternative.

Chapter 6: General Discussion and Conclusions

6.1 General Discussion

The main objectives of this thesis were to optimize a loop-mediated isothermal amplification reaction for the detection of *stx*$_1$ and *stx*$_2$ in clinical stool samples and compare its performance to that of the current method used at the Provincial Laboratory in Edmonton, real-time PCR. Comparisons to conventional PCR were not performed for clinical samples, as this method is not used at the Provincial Laboratory for STEC testing. A further goal of the study was to eliminate the need for agarose gel electrophoresis product detection as a way to increase the simplicity of the assay, as well as to decrease the total cost associated with the test. As an extension of the study, the opportunity to test the Genie II automated LAMP reader arose, and this system was tested with the panel of blinded clinical samples used for the initial optimized LAMP reaction.

Finding the ideal conditions of time, temperature, magnesium concentration and enzyme concentration for both primer sets successfully optimized the LAMP assay. Contrary to some previous studies, betaine was not sufficient to denature template DNA; heat denaturation was required to eliminate the production of artifact and increase reaction sensitivity (108). Other studies have obtained similar unsatisfactory results when relying solely on a chemical denaturant, such as betaine, for template denaturation, as such the need for heat denaturation is likely primer set-dependent (134). Once optimized, the assay cost per 10 reactions, sensitivity, and specificity of LAMP assay were comparable to the gold standard RT-PCR. LAMP had a turn-around-time of 3 hours versus 65 minutes for RT-PCR due to the need for agarose gel electrophoresis product detection.

Testing the optimized LAMP assay using agarose gel electrophoresis product detection with a panel of blinded clinical stool samples revealed that the assay is susceptible to contamination; likely due to the high sensitivity of the reaction and open tube system. The sensitivity of LAMP was 90%/100%, specificity 95%/99%, positive predictive value 56%/89%, and negative predictive

value 99%/100% for *stx*$_1$ and *stx*$_{2,}$ respectively. All false positive results were resolved after 1 repeat, pointing towards environmental contamination as the cause. Overall, the results obtained with LAMP were comparable to those of RT-PCR; however, it is recommended to repeat testing on any positive samples to rule out the possibility of false positives.

To eliminate the need for agarose gel electrophoresis to detect LAMP amplification products, a Sybr Green I detection system was developed. When Sybr Green I intercalates with double stranded DNA the reaction visibly turns from orange to green, and fluoresces green under UV light (137). The downside of the SG1 detection system developed in this study is that it is not a closed tube system. As SG1 detects all double-stranded DNA, it will give positive results in the presence of amplicons that contaminate the reaction upon the opening of reaction tubes. As such, false positives were observed when testing SG1 with clinical samples in this study. The high rate of false positivity led to sensitivities of 100/100%, specificities of 93/77%, positive predictive values of 76/39% and negative predictive values of 100/100% for *stx*$_1$ and *stx*$_2$ respectively. In many cases, concordance was never achieved, even upon multiple repeats as the extreme sensitivity of the LAMP reaction combined with SG1 detection led to contaminating amplicons being detected, which caused false positive results.

When the Genie II was tested with the same clinical panel, only one false positive result was obtained, and it was resolved upon one repeat. The Genie II is much less susceptible to contamination as it is a completely closed tube system, once the reaction has been set up, reaction tubes are not opened for product detection as the automated reader measures fluorescence as the reaction progresses (129). Although the Genie II appears to produce more reliable results than an open-tube LAMP system, it does have its disadvantages including higher cost and requirement for computer connectivity. As the Genie II was only briefly investigated, further study would be required to fully assess its suitability for clinical diagnostic testing.

6.2 Limitations of this Study

The main limitation of this study is the use of 5 µL of template for RT-PCR in the clinical sample testing phase and 3 µL of template for LAMP. The RT-PCR results were obtained as part of a previous study, where 5 µL of template in a 25 µL total reaction volume was required as per the standardized protocol. In order to maintain a total reaction volume of 25 µL for the optimized LAMP assay, only 3 µL of template could be used, as this is the maximum amount of water that could be removed from the reaction. Ideally, 3 µL of reaction template would have also been used for RT-PCR. However, the LAMP results compared well with those of RT-PCR and that the main issue was not false negatives, but false positives. This indicates that using less template DNA for LAMP did not hinder the assay's ability to detect positive reactions as compared to RT-PCR. If anything LAMPs higher degree of sensitivity led to an increase in false positive results.

6.3 Final Conclusions

Once the LAMP assay has been converted into a closed tube system, it will be an ideal assay for use in all environments, from large hospitals to small rural laboratories. As a closed tube system, LAMP would meet the ASSURED criteria for laboratory tests in areas of limited resources of **A**ffordability, **S**ensitivity, **S**pecificity, **U**ser-friendliness, **R**apidity and robustness, freedom from **E**quipment, and **D**eliverability (98, 100). As such, LAMP assays represent a way of bringing highly accurate molecular testing to areas of the world that currently have little to no means of accurate laboratory testing. LAMP assays have a vast potential to simplify molecular testing for laboratories of all sizes and means. The LAMP assay using agarose gel electrophoresis product detection developed in this study represents a possibility for *stx* testing in all environments; as long as positive reactions are confirmed by repeat testing. The LAMP assay using Sybr Green 1 product detection is currently un-reliable for clinical diagnostic work; however, if the assay can be converted to a closed-tube system it will be an ideal testing method.

6.4 Future Work

Development of a completely closed tube LAMP assay would be very beneficial and as such warrant further study. A closed tube method of product detection would likely significantly decrease the incidence of false positive results, and thus increase the reliability and user-friendliness of the assay. The major difficulty that must be considered is the inhibition of the *Bst* polymerase enzyme in the LAMP assays by Sybr Green I. A method of adding Sybr Green I at the beginning of the reaction but not allowing it to participate in reaction until amplification is complete must be devised. Once the closed tube method was developed, it would require testing with another blinded panel of clinical stool samples in order to evaluate its performance.

Appendix

Sample Primer Calculation:

93.1 nmol in 100µL = 0.931 nmol/µL = 931 pmol/ µL

(931pmol/ µL)(V_1) = (20pmol/ µL)(200 µL)

V_1 = 4.3 µL in 195.7 µL of H_2O

Calculation of CFU/mL in 0.5 OD Cell Suspension:

$$\frac{47}{0.01\text{mL}} = \frac{x}{1\text{mL}} = 4700 \text{ CFU/mL}$$

In the 10^{-4} dilution 4700 CFU/mL were present, therefore the original undiluted 0.5 OD specimen contained 4.7×10^7 CFU/mL or 0.5×10^8 CFU/mL. The results of this experiment were confirmed upon repeat.

Calculation of Sensitivity using Dilution Panel:

Cell suspensions of 0.5 O.D have been shown to contain approximately 10^8 CFU/mL. As each 200 µL of each cell suspension was eluted into 200 µL of elution buffer the CFU present in each DNA extract is as follows:

10^{-1} Dilution = 10^7 CFU/mL = 10 000 CFU
10^{-2} Dilution = 10^6 CFU/mL = 1000 CFU
10^{-3} Dilution = 10^5 CFU/mL = 100 CFU
10^{-4} Dilution = 10^4 CFU/mL = 10 CFU
10^{-5} Dilution = 10^3 CFU/mL = 1 CFU
10^{-6} Dilution = 10^2 CFU/mL = 1 CFU
10^{-7} Dilution = 10^1 CFU/mL = 1 CFU
10^{-8} Dilution = 10^0 CFU/mL = 1 CFU

Sample Calculation:

$$\frac{10^3 \text{ CFU}}{1000 \text{ µL}} \times \frac{200 \text{ µL}}{200 \text{ µL}} = 1 \text{ CFU}$$

References

(1) Nataro JP, Kaper JB. Diarrheagenic Escherichia coli. Clin Microbiol Rev 1998 Jan;11(1):142-201.

(2) Tarr PI. Escherichia coli O157:H7: clinical, diagnostic, and epidemiological aspects of human infection. Clin Infect Dis 1995 quiz 9-10; Jan;20(1):1-8.

(3) Pennington H. Escherichia coli O157. Lancet 2010 Oct 23;376(9750):1428-1435.

(4) Tarr PI, Fouser LS, Stapleton AE, Wilson RA, Kim HH, Vary JC,Jr, et al. Hemolytic-uremic syndrome in a six-year-old girl after a urinary tract infection with Shiga-toxin-producing Escherichia coli O103:H2. N Engl J Med 1996 Aug 29;335(9):635-638.

(5) Karmali MA. Infection by verocytotoxin-producing Escherichia coli. Clin Microbiol Rev 1989 Jan;2(1):15-38.

(6) Rangel JM, Sparling PH, Crowe C, Griffin PM, Swerdlow DL. Epidemiology of Escherichia coli O157:H7 outbreaks, United States, 1982-2002. Emerg Infect Dis 2005 Apr;11(4):603-609.

(7) Gould LH. Bopp C. Strockbine N. Atkinson R. Baselski V. Body B. Carey R. Crandall C. Hurd S. Kaplan R. Neill M. Shea S. Somsel P. Tobin-D'Angelo M. Griffin PM. Gerner-Smidt P. Centers for Disease Control and Prevention (CDC). Recommendations for diagnosis of shiga toxin--producing Escherichia coli infections by clinical laboratories. MMWR Recomm Rep 2009 Oct 16;58(RR-12):1-14.

(8) Olmsted SS, Moore M, Meili RC, Duber HC, Wasserman J, Sama P, et al. Strengthening laboratory systems in resource-limited settings. Am J Clin Pathol 2010 Sep;134(3):374-380.

(9) Berg H. E.coli in Motion. New York: Springer; 2004.

(10) Evans D, Evans D. Chapter 25: Escherichia coli in Diarrheal Disease. In: Baron S, editor. Medical Microbiology. 4th ed. Galveston, Texas: University of Texas Medical Branch at Galveston; 1996.

(11) Riley LW, Remis RS, Helgerson SD, McGee HB, Wells JG, Davis BR, et al. Hemorrhagic colitis associated with a rare Escherichia coli serotype. N Engl J Med 1983 Mar 24;308(12):681-685.

(12) Neil KP, Biggerstaff G, MacDonald JK, Trees E, Medus C, Musser KA, et al. A novel vehicle for transmission of Escherichia coli O157:H7 to humans:

multistate outbreak of E. coli O157:H7 infections associated with consumption of ready-to-bake commercial prepackaged cookie dough--United States, 2009. Clin Infect Dis 2012 Feb 15;54(4):511-518.

(13) Gaulin C, Levac E, Ramsay D, Dion R, Ismail J, Gingras S, et al. Escherichia coli O157:H7 outbreak linked to raw milk cheese in Quebec, Canada: use of exact probability calculation and casecase study approaches to foodborne outbreak investigation. J Food Prot 2012 May;75(5):812-818.

(14) Miller BD, Rigdon CE, Ball J, Rounds JM, Klos RF, Brennan BM, et al. Use of traceback methods to confirm the source of a multistate Escherichia coli O157:H7 outbreak due to in-shell hazelnuts. J Food Prot 2012 Feb;75(2):320-327.

(15) Centers for Disease Control and Prevention (CDC). Notes from the field: Escherichia coli O157:H7 gastroenteritis associated with a State Fair - North Carolina, 2011. MMWR Morb Mortal Wkly Rep 2012 Jan 6;60(51-52):1745-1746.

(16) Matsell DG, White CT. An outbreak of diarrhea-associated childhood hemolytic uremic syndrome: the Walkerton epidemic. Kidney Int Suppl 2009 Feb(112):S35-7.

(17) Salvadori MI, Sontrop JM, Garg AX, Moist LM, Suri RS, Clark WF. Factors that led to the Walkerton tragedy. Kidney Int Suppl 2009 Feb(112):S33-4.

(18) Brown JA, Hite DS, Gillim-Ross LA, Maguire HF, Bennett JK, Patterson JJ, et al. Outbreak of shiga toxin-producing Escherichia coli serotype O26: H11 infection at a child care center in Colorado. Pediatr Infect Dis J 2012 Apr;31(4):379-383.

(19) Centers for Disease Control and Prevention (CDC). Outbreak of Shiga toxin-producing Escherichia coli O111 infections associated with a correctional facility dairy - Colorado, 2010. MMWR Morb Mortal Wkly Rep 2012 Mar 9;61(9):149-152.

(20) Beutin L, Martin A. Outbreak of Shiga toxin-producing Escherichia coli (STEC) O104:H4 infection in Germany causes a paradigm shift with regard to human pathogenicity of STEC strains. J Food Prot 2012 Feb;75(2):408-418.

(21) Folster JP, Pecic G, Taylor E, Whichard J. Characterization of Isolates from an outbreak of multidrug-resistant, Shiga toxin-producing Escherichia coli O145 in the United States. Antimicrob Agents Chemother 2011 Dec;55(12):5955-5956.

(22) Schaffzin JK, Coronado F, Dumas NB, Root TP, Halse TA, Schoonmaker-Bopp DJ, et al. Public health approach to detection of non-O157 Shiga toxin-

producing Escherichia coli: summary of two outbreaks and laboratory procedures. Epidemiol Infect 2012 Feb;140(2):283-289.

(23) Alexander DC, Hao W, Gilmour MW, Zittermann S, Sarabia A, Melano RG, et al. Escherichia coli O104:H4 infections and international travel. Emerg Infect Dis 2012 Mar;18(3):473-476.

(24) Public Health Agency of Canada. E.coli Fact Sheet. 2013; Available at: http://www.phac-aspc.gc.ca/fs-sa/fs-fi/ecoli-eng.php. Accessed June/13, 2013.

(25) Vally H, Hall G, Dyda A, Raupach J, Knope K, Combs B, et al. Epidemiology of Shiga toxin producing Escherichia coli in Australia, 2000-2010. BMC Public Health 2012;12:63.

(26) Evans J, Knight H, McKendrick IJ, Stevenson H, Varo Barbudo A, Gunn GJ, et al. Prevalence of Escherichia coli O157: H7 and serogroups O26, O103, O111 and O145 in sheep presented for slaughter in Scotland. J Med Microbiol 2011 May;60(Pt 5):653-660.

(27) Ferens WA, Hovde CJ. Escherichia coli O157:H7: animal reservoir and sources of human infection. Foodborne Pathog Dis 2011 Apr;8(4):465-487.

(28) Zhang XS, Woolhouse ME. Escherichia coli O157 infection on Scottish cattle farms: dynamics and control. J R Soc Interface 2011 Jul 6;8(60):1051-1058.

(29) Berger CN, Sodha SV, Shaw RK, Griffin PM, Pink D, Hand P, et al. Fresh fruit and vegetables as vehicles for the transmission of human pathogens. Environ Microbiol 2010 Sep;12(9):2385-2397.

(30) Buchholz U, Bernard H, Werber D, Bohmer MM, Remschmidt C, Wilking H, et al. German outbreak of Escherichia coli O104:H4 associated with sprouts. N Engl J Med 2011 Nov 10;365(19):1763-1770.

(31) Denny J, Bhat M, Eckmann K. Outbreak of Escherichia coli O157:H7 associated with raw milk consumption in the Pacific Northwest. Foodborne Pathog Dis 2008 Jun;5(3):321-328.

(32) Ethelberg S, Smith B, Torpdahl M, Lisby M, Boel J, Jensen T, et al. Outbreak of non-O157 Shiga toxin-producing Escherichia coli infection from consumption of beef sausage. Clin Infect Dis 2009 Apr 15;48(8):e78-81.

(33) Grant J, Wendelboe AM, Wendel A, Jepson B, Torres P, Smelser C, et al. Spinach-associated Escherichia coli O157:H7 outbreak, Utah and New Mexico, 2006. Emerg Infect Dis 2008 Oct;14(10):1633-1636.

(34) King LA, Mailles A, Mariani-Kurkdjian P, Vernozy-Rozand C, Montet MP, Grimont F, et al. Community-wide outbreak of Escherichia coli O157:H7 associated with consumption of frozen beef burgers. Epidemiol Infect 2009 Jun;137(6):889-896.

(35) Pu S, Beaulieu JC, Prinyawiwatkul W, Ge B. Effects of plant maturity and growth media bacterial inoculum level on the surface contamination and internalization of Escherichia coli O157:H7 in growing spinach leaves. J Food Prot 2009 Nov;72(11):2313-2320.

(36) Mather AE, Reid SW, McEwen SA, Ternent HE, Reid-Smith RJ, Boerlin P, et al. Factors associated with cross-contamination of hides of Scottish cattle by Escherichia coli O157. Appl Environ Microbiol 2008 Oct;74(20):6313-6319.

(37) Mather AE, Innocent GT, McEwen SA, Reilly WJ, Taylor DJ, Steele WB, et al. Risk factors for hide contamination of Scottish cattle at slaughter with Escherichia coli O157. Prev Vet Med 2007 Aug 16;80(4):257-270.

(38) Arthur TM, Keen JE, Bosilevac JM, Brichta-Harhay DM, Kalchayanand N, Shackelford SD, et al. Longitudinal study of Escherichia coli O157:H7 in a beef cattle feedlot and role of high-level shedders in hide contamination. Appl Environ Microbiol 2009 Oct;75(20):6515-6523.

(39) Chapman PA, Siddons CA, Wright DJ, Norman P, Fox J, Crick E. Cattle as a possible source of verocytotoxin-producing Escherichia coli O157 infections in man. Epidemiol Infect 1993 Dec;111(3):439-447.

(40) Elder RO, Keen JE, Siragusa GR, Barkocy-Gallagher GA, Koohmaraie M, Laegreid WW. Correlation of enterohemorrhagic Escherichia coli O157 prevalence in feces, hides, and carcasses of beef cattle during processing. Proc Natl Acad Sci U S A 2000 Mar 28;97(7):2999-3003.

(41) Auld H, MacIver D, Klaassen J. Heavy rainfall and waterborne disease outbreaks: the Walkerton example. J Toxicol Environ Health A 2004 Oct 22-;67(20-22):1879-1887.

(42) Clark WF, Sontrop JM, Macnab JJ, Salvadori M, Moist L, Suri R, et al. Long term risk for hypertension, renal impairment, and cardiovascular disease after gastroenteritis from drinking water contaminated with Escherichia coli O157:H7: a prospective cohort study. BMJ 2010;341:6020.

(43) Friedman MS, Roels T, Koehler JE, Feldman L, Bibb WF, Blake P. Escherichia coli O157:H7 outbreak associated with an improperly chlorinated swimming pool. Clin Infect Dis 1999 Aug;29(2):298-303.

(44) Crump JA, Sulka AC, Langer AJ, Schaben C, Crielly AS, Gage R, et al. An outbreak of Escherichia coli O157:H7 infections among visitors to a dairy farm. N Engl J Med 2002 Aug 22;347(8):555-560.

(45) Centers for Disease Control and Prevention (CDC). Outbreak of Shiga toxin-producing Escherichia coli O157 infection associated with a day camp petting zoo--Pinellas County, Florida, May-June 2007. MMWR Morb Mortal Wkly Rep 2009 May 1;58(16):426-428.

(46) Heuvelink AE, van Heerwaarden C, Zwartkruis-Nahuis JT, van Oosterom R, Edink K, van Duynhoven YT, et al. Escherichia coli O157 infection associated with a petting zoo. Epidemiol Infect 2002 Oct;129(2):295-302.

(47) Boudailliez B, Berquin P, Mariani-Kurkdjian P, Ilef D, Cuvelier B, Capek I, et al. Possible person-to-person transmission of Escherichia coli O111--associated hemolytic uremic syndrome. Pediatr Nephrol 1997 Feb;11(1):36-39.

(48) Gilbert M, Monk C, Wang HL, Diplock K, Landry L. Screening policies for daycare attendees: lessons learned from an outbreak of E. coli O157:H7 in a daycare in Waterloo, Ontario. Can J Public Health 2008 Jul-Aug;99(4):281-285.

(49) Aldabe B, Delmas Y, Gault G, Vendrely B, Llanas B, Charron M, et al. Household transmission of haemolytic uraemic syndrome associated with Escherichia coli O104:H4, south-western France, June 2011. Euro Surveillance: Bulletin Europeen sur les Maladies Transmissibles = European Communicable Disease Bulletin 2011;16(31).

(50) Seto EY, Soller JA, Colford JM,Jr. Strategies to reduce person-to-person transmission during widespread Escherichia coli O157:H7 outbreak. Emerg Infect Dis 2007 Jun;13(6):860-866.

(51) Vaillant V, Espie E, de Valk H, Durr U, Barataud D, Bouvet P, et al. Undercooked ground beef and person-to-person transmission as major risk factors for sporadic hemolytic uremic syndrome related to Shiga-toxin producing Escherchia coli infections in children in France. Pediatr Infect Dis J 2009 Jul;28(7):650-653.

(52) Tuttle J, Gomez T, Doyle MP, Wells JG, Zhao T, Tauxe RV, et al. Lessons from a large outbreak of Escherichia coli O157:H7 infections: insights into the infectious dose and method of widespread contamination of hamburger patties. Epidemiol Infect 1999 Apr;122(2):185-192.

(53) Bentancor AB, Ameal LA, Calvino MF, Martinez MC, Miccio L, Degregorio OJ. Risk factors for Shiga toxin-producing Escherichia coli infections in preadolescent schoolchildren in Buenos Aires, Argentina. J infect dev ctries 2012 May;6(5):378-386.

(54) Reilly A. Prevention and control of enterohaemorrhagic Escherichia coli (EHEC) infections: memorandum from a WHO meeting. WHO Consultation on Prevention and Control of Enterohaemorrhagic Escherichia coli (EHEC) Infections. Bull World Health Organ 1998;76(3):245-255.

(55) Chapter 17: Shiga Toxins of Shigella dysenteriae and Escherichia coli. In: Aktories K, Just I, editors. Handbook of Experimental Pharmacology: Bacterial Protein Toxins Germany: Springer. p. 385-406.

(56) Ling H, Boodhoo A, Hazes B, Cummings MD, Armstrong GD, Brunton JL, et al. Structure of the shiga-like toxin I B-pentamer complexed with an analogue of its receptor Gb3. Biochemistry 1998 Feb 17;37(7):1777-1788.

(57) Gallegos KM, Conrady DG, Karve SS, Gunasekera TS, Herr AB, Weiss AA. Shiga toxin binding to glycolipids and glycans. PLoS ONE 2012;7(2):e30368.

(58) Fraser ME, Fujinaga M, Cherney MM, Melton-Celsa AR, Twiddy EM, O'Brien AD, et al. Structure of shiga toxin type 2 (Stx2) from Escherichia coli O157:H7. J Biol Chem 2004 Jun 25;279(26):27511-27517.

(59) Fraser ME, Chernaia MM, Kozlov YV, James MN. Crystal structure of the holotoxin from Shigella dysenteriae at 2.5 A resolution. Nat Struct Biol 1994 Jan;1(1):59-64.

(60) The Shiga Toxins: Properties and Actions on cells. In: Alouf J, editor. The Comprehensive Sourcebook of Bacterial Protein Toxins. 3rd ed.: Elsevier; 2006. p. 310-322.

(61) Beddoe T, Paton AW, Le Nours J, Rossjohn J, Paton JC. Structure, biological functions and applications of the AB5 toxins. Trends Biochem Sci 2010 Jul;35(7):411-418.

(62) Kurmanova A, Llorente A, Polesskaya A, Garred O, Olsnes S, Kozlov J, et al. Structural requirements for furin-induced cleavage and activation of Shiga toxin. Biochem Biophys Res Commun 2007 May 25;357(1):144-149.

(63) Boyd B, Tyrrell G, Maloney M, Gyles C, Brunton J, Lingwood C. Alteration of the glycolipid binding specificity of the pig edema toxin from globotetraosyl to globotriaosyl ceramide alters in vivo tissue targetting and results in a verotoxin 1-like disease in pigs. J Exp Med 1993 Jun 1;177(6):1745-1753.

(64) Kuczius T, Bielaszewska M, Friedrich AW, Zhang W. A rapid method for the discrimination of genes encoding classical Shiga toxin (Stx) 1 and its variants, Stx1c and Stx1d, in Escherichia coli. Mol Nutr Food Res 2004 Dec;48(7):515-521.

(65) Feng PC, Jinneman K, Scheutz F, Monday SR. Specificity of PCR and serological assays in the detection of Escherichia coli Shiga toxin subtypes. Appl Environ Microbiol 2011 Sep;77(18):6699-6702.

(66) Li R, Harada T, Honjoh K, Miyamoto T. Phylogenetic analysis and Shiga toxin production profiling of Shiga toxin-producing/enterohemorrhagic Escherichia coli clinical isolates. Microb Pathog 2010 Nov;49(5):246-251.

(67) Friedrich AW, Bielaszewska M, Zhang WL, Pulz M, Kuczius T, Ammon A, et al. Escherichia coli harboring Shiga toxin 2 gene variants: frequency and association with clinical symptoms. J Infect Dis 2002 Jan 1;185(1):74-84.

(68) DeGrandis S, Law H, Brunton J, Gyles C, Lingwood CA. Globotetraosylceramide is recognized by the pig edema disease toxin. J Biol Chem 1989 Jul 25;264(21):12520-12525.

(69) Lea N, Lord JM, Roberts LM. Proteolytic cleavage of the A subunit is essential for maximal cytotoxicity of Escherichia coli O157:H7 Shiga-like toxin-1. Microbiology 1999 May;145(Pt 5):999-1004.

(70) Cookson AL, Bennett J, Thomson-Carter F, Attwood GT. Molecular subtyping and genetic analysis of the enterohemolysin gene (ehxA) from Shiga toxin-producing escherichia coli and atypical enteropathogenic E. coli. Appl Environ Microbiol 2007 Oct;73(20):6360-6369.

(71) Law D. Virulence factors of Escherichia coli O157 and other Shiga toxin-producing E. coli. J Appl Microbiol 2000 May;88(5):729-745.

(72) Farfan MJ, Torres AG. Molecular mechanisms that mediate colonization of Shiga toxin-producing Escherichia coli strains. Infect Immun 2012 Mar;80(3):903-913.

(73) Fitzhenry RJ, Pickard DJ, Hartland EL, Reece S, Dougan G, Phillips AD, et al. Intimin type influences the site of human intestinal mucosal colonisation by enterohaemorrhagic Escherichia coli O157:H7. Gut 2002 Feb;50(2):180-185.

(74) Michel PA, Kase JA. Genetic profiles of Shiga toxin and intimin genes found in stool broth cultures: a 2-year reference laboratory study. Diagn Microbiol Infect Dis 2009 Oct;65(2):85-92.

(75) Ross NT, Miller BL. Characterization of the binding surface of the translocated intimin receptor, an essential protein for EPEC and EHEC cell adhesion. Protein Sci 2007 Dec;16(12):2677-2683.

(76) Girard F, Dziva F, van Diemen P, Phillips AD, Stevens MP, Frankel G. Adherence of enterohemorrhagic Escherichia coli O157, O26, and O111 strains

to bovine intestinal explants ex vivo. Appl Environ Microbiol 2007 May;73(9):3084-3090.

(77) Yi Y, Ma Y, Gao F, Mao X, Peng H, Feng Y, et al. Crystal structure of EHEC intimin: insights into the complementarity between EPEC and EHEC. PLoS ONE 2010;5(12):e15285.

(78) Sinclair JF, Dean-Nystrom EA, O'Brien AD. The established intimin receptor Tir and the putative eucaryotic intimin receptors nucleolin and beta1 integrin localize at or near the site of enterohemorrhagic Escherichia coli O157:H7 adherence to enterocytes in vivo. Infect Immun 2006 Feb;74(2):1255-1265.

(79) Feng PC, Keys C, Lacher D, Monday SR, Shelton D, Rozand C, et al. Prevalence, characterization and clonal analysis of Escherichia coli O157: non-H7 serotypes that carry eae alleles. FEMS Microbiol Lett 2010 Jul 1;308(1):62-67.

(80) Karpman D, Sartz L, Johnson S. Pathophysiology of typical hemolytic uremic syndrome. Semin Thromb Hemost 2010 Sep;36(6):575-585.

(81) Banatvala N, Griffin PM, Greene KD, Barrett TJ, Bibb WF, Green JH, et al. The United States National Prospective Hemolytic Uremic Syndrome Study: microbiologic, serologic, clinical, and epidemiologic findings. J Infect Dis 2001 Apr 1;183(7):1063-1070.

(82) Caprioli A, Luzzi I, Rosmini F, Resti C, Edefonti A, Perfumo F, et al. Community-wide outbreak of hemolytic-uremic syndrome associated with non-O157 verocytotoxin-producing Escherichia coli. J Infect Dis 1994 Jan;169(1):208-211.

(83) Griffin PM, Tauxe RV. The epidemiology of infections caused by Escherichia coli O157:H7, other enterohemorrhagic E. coli, and the associated hemolytic uremic syndrome. Epidemiol Rev 1991;13:60-98.

(84) Bekassy ZD, Calderon Toledo C, Leoj G, Kristoffersson A, Leopold SR, Perez MT, et al. Intestinal damage in enterohemorrhagic Escherichia coli infection. Pediatr Nephrol 2011 Nov;26(11):2059-2071.

(85) Bowles C, Ancker M, Triadafilopoulos G. Gastrointestinal dysfunction following hemolytic uremic syndrome. Dig Dis Sci 2011 Aug;56(8):2241-2243.

(86) Hettiarachchi IT, Hegde M, Planner AC, John L. Escherichia coli O157:H7 causing hemorrhagic colitis. Gastrointest Endosc 2012 discussion 675; Mar;75(3):674-675.

(87) Ray PE, Liu XH. Pathogenesis of Shiga toxin-induced hemolytic uremic syndrome. Pediatr Nephrol 2001 Oct;16(10):823-839.

(88) Goldwater PN, Bettelheim KA. Treatment of enterohemorrhagic Escherichia coli (EHEC) infection and hemolytic uremic syndrome (HUS). BMC Med 2012;10:12.

(89) Loirat C, Saland J, Bitzan M. Management of hemolytic uremic syndrome. Presse Med 2012 Mar;41(3 Pt 2):e115-35.

(90) Hoefer D, Hurd S, Medus C, Cronquist A, Hanna S, Hatch J, et al. Laboratory practices for the identification of Shiga toxin-producing Escherichia coli in the United States, FoodNet sites, 2007. Foodborne Pathog Dis 2011 Apr;8(4):555-560.

(91) March SB, Ratnam S. Sorbitol-MacConkey medium for detection of Escherichia coli O157:H7 associated with hemorrhagic colitis. J Clin Microbiol 1986 May;23(5):869-872.

(92) Hirvonen JJ, Siitonen A, Kaukoranta SS. Usability and Performance of CHROMagar STEC Medium in Detection of Shiga Toxin-Producing Escherichia coli Strains. J Clin Microbiol 2012 Nov;50(11):3586-3590.

(93) Church DL, Emshey D, Semeniuk H, Lloyd T, Pitout JD. Evaluation of BBL CHROMagar O157 versus sorbitol-MacConkey medium for routine detection of Escherichia coli O157 in a centralized regional clinical microbiology laboratory. J Clin Microbiol 2007 Sep;45(9):3098-3100.

(94) Bettelheim KA. Reliability of CHROMagar O157 for the detection of enterohaemorrhagic Escherichia coli (EHEC) O157 but not EHEC belonging to other serogroups. J Appl Microbiol 1998 Sep;85(3):425-428.

(95) Gouali M, Ruckly C, Carle I, Lejay-Collin M, Weill FX. Evaluation of CHROMagar STEC and STEC O104 chromogenic agar media for detection of Shiga Toxin-producing Escherichia coli in stool specimens. J Clin Microbiol 2013 Mar;51(3):894-900.

(96) Wylie JL, Van Caeseele P, Gilmour MW, Sitter D, Guttek C, Giercke S. Evaluation of a new chromogenic agar medium for detection of Shiga toxin-producing Escherichia coli (STEC) and relative prevalences of O157 and non-O157 STEC in Manitoba, Canada. J Clin Microbiol 2013 Feb;51(2):466-471.

(97) Klein EJ, Stapp JR, Neill MA, Besser JM, Osterholm MT, Tarr PI. Shiga toxin antigen detection should not replace sorbitol MacConkey agar screening of stool specimens. J Clin Microbiol 2004 author reply 4416-7; Sep;42(9):4416-7.

(98) Peeling RW, Holmes KK, Mabey D, Ronald A. Rapid tests for sexually transmitted infections (STIs): the way forward. Sex Transm Infect 2006 December;82(Supplement 5):1-6.

(99) Donegan E, Moncada J, Chernesky M, Schachter J. Sexually transmitted infection/HIV laboratory testing in resource-limited countries: steps to improve use effective testing and to ensure diagnostic capacity. Sex Transm Dis 2003 Dec;30(12):905-908.

(100) Kosack CS. Experience of Medecins Sans Frontieres in laboratory medicine in resource-limited settings. Clin Chem Lab Med 2012 Jul;50(7):1221-1227.

(101) Martin R, Barnhart S. Global laboratory systems development: needs and approaches. Infect Dis Clin North Am 2011 x; Sep;25(3):677-691.

(102) Notomi T, Okayama H, Masubuchi H, Yonekawa T, Watanabe K, Amino N, et al. Loop-mediated isothermal amplification of DNA. Nucleic Acids Res 2000 Jun 15;28(12):E63.

(103) Nagamine K, Hase T, Notomi T. Accelerated reaction by loop-mediated isothermal amplification using loop primers. Molecular & Cellular Probes 2002 Jun;16(3):223-229.

(104) Eiken Chemical. Primer Explorer: LAMP primer designing software. 2005; Available at: http://primerexplorer.jp/e/, 2012.

(105) Eiken Chemical. The principle of LAMP Method: Design of Primers. 2005; Available at: http://loopamp.eiken.co.jp/e/lamp/primer.html. Accessed Sept/11, 2012.

(106) Aliotta JM, Pelletier JJ, Ware JL, Moran LS, Benner JS, Kong H. Thermostable Bst DNA polymerase I lacks a 3'-->5' proofreading exonuclease activity. Genet Anal 1996 Mar;12(5-6):185-195.

(107) New England Biolabs. *Bst*DNA Polymerase, Large Fragment. Available at: http://www.neb.com/nebecomm/products/productm0275.asp, 2012.

(108) Nagamine K, Watanabe K, Ohtsuka K, Hase T, Notomi T. Loop-mediated isothermal amplification reaction using a nondenatured template. Clin Chem 2001 Sep;47(9):1742-1743.

(109) Mori Y, Nagamine K, Tomita N, Notomi T. Detection of loop-mediated isothermal amplification reaction by turbidity derived from magnesium pyrophosphate formation. Biochemical & Biophysical Research Communications 2001 Nov 23;289(1):150-154.

(110) Mori Y, Kitao M, Tomita N, Notomi T. Real-time turbidimetry of LAMP reaction for quantifying template DNA. Journal of Biochemical & Biophysical Methods 2004 May 31;59(2):145-157.

(111) Goto M, Honda E, Ogura A, Nomoto A, Hanaki K. Colorimetric detection of loop-mediated isothermal amplification reaction by using hydroxy naphthol blue. BioTechniques 2009 Mar;46(3):167-172.

(112) Wastling SL, Picozzi K, Kakembo AS, Welburn SC. LAMP for human African trypanosomiasis: a comparative study of detection formats. PLoS Negl Trop Dis 2010;4(11):e865.

(113) Tomita N, Mori Y, Kanda H, Notomi T. Loop-mediated isothermal amplification (LAMP) of gene sequences and simple visual detection of products. Nat protoc 2008;3(5):877-882.

(114) Roche Diagnostics. LightCycler 480 SYBR Green I Master. Available at: http://www.roche-applied-science.com/proddata/gpip/3_5_8_1_1_2.html. Accessed Nov/11, 2012.

(115) Hong M, Zha L, Fu W, Zou M, Li W, Xu D. A modified visual loop-mediated isothermal amplification method for diagnosis and differentiation of main pathogens from Mycobacterium tuberculosis complex. World J Microbiol Biotechnol 2012 Feb;28(2):523-531.

(116) Matsui K, Ishii N, Honjo M, Kawabata Z. Use of the SYBR Green I fluorescent dye and a centrifugal filter device for rapid determination of
dissolved DNA concentration in fresh water. Aquat Microb Ecol 2004;36:99-105.

(117) Tao ZY, Zhou HY, Xia H, Xu S, Zhu HW, Culleton RL, et al. Adaptation of a visualized loop-mediated isothermal amplification technique for field detection of Plasmodium vivax infection. Parasit Vectors 2011;4:115.

(118) Abdul-Ghani R, Al-Mekhlafi AM, Karanis P. Loop-mediated isothermal amplification (LAMP) for malarial parasites of humans: would it come to clinical reality as a point-of-care test?. Acta Trop 2012 Jun;122(3):233-240.

(119) Njiru ZK. Loop-mediated isothermal amplification technology: towards point of care diagnostics. PLoS Negl Trop Dis 2012 Jun;6(6):e1572.

(120) Hara-Kudo Y, Nemoto J, Ohtsuka K, Segawa Y, Takatori K, Kojima T, et al. Sensitive and rapid detection of Vero toxin-producing Escherichia coli using loop-mediated isothermal amplification. J Med Microbiol 2007 Mar;56(Pt 3):398-406.

(121) Wang F, Jiang L, Ge B. Loop-mediated isothermal amplification assays for detecting shiga toxin-producing Escherichia coli in ground beef and human stools. J Clin Microbiol 2012 Jan;50(1):91-97.

(122) Francois P, Tangomo M, Hibbs J, Bonetti EJ, Boehme CC, Notomi T, et al. Robustness of a loop-mediated isothermal amplification reaction for diagnostic applications. FEMS Immunology & Medical Microbiology 2011 Jun;62(1):41-48.

(123) Cai SH, Wang B, Lu YS, Jian JC, Wu ZH. Development of Loop-mediated isothermal amplification method for rapid detection of Streptococcus iniae, the causative agent of streptococcicosis in fish. J Basic Microbiol 2012 Apr;52(2):116-122.

(124) Aryan E, Makvandi M, Farajzadeh A, Huygen K, Bifani P, Mousavi SL, et al. A novel and more sensitive loop-mediated isothermal amplification assay targeting IS6110 for detection of Mycobacterium tuberculosis complex. Microbiol Res 2010 Mar 31;165(3):211-220.

(125) Tao ZY, Zhou HY, Xia H, Xu S, Zhu HW, Culleton RL, et al. Adaptation of a visualized loop-mediated isothermal amplification technique for field detection of Plasmodium vivax infection. Parasites & Vectors [Electronic Resource] 2011;4:115.

(126) Iwamoto T, Sonobe T, Hayashi K. Loop-mediated isothermal amplification for direct detection of Mycobacterium tuberculosis complex, M. avium, and M. intracellulare in sputum samples. J Clin Microbiol 2003 Jun;41(6):2616-2622.

(127) Tang Y, Diao Y, Yu C, Gao X, Chen L, Zhang D. Rapid Detection of Tembusu Virus by Reverse-Transcription, Loop-mediated Isothermal Amplification (RT-LAMP). Transboundary & Emerging Diseases 2012 Jun;59(3):208-213.

(128) Eiken Chemical. Loopamp Real-time Turbidimeter (LA-500). 2005; Available at: http://loopamp.eiken.co.jp/e/products/la500/index.html. Accessed Feb/14, 2013.

(129) Optigene. Genie II User Manual. ;vs 1.08.

(130) Promega. Technical Bulletin: MagaZorb® DNA Mini-Prep Kit. 2011.

(131) Chui L, Couturier MR, Chiu T, Wang G, Olson AB, McDonald RR, et al. Comparison of Shiga toxin-producing Escherichia coli detection methods using clinical stool samples. J Mol Diagn 2010 Jul;12(4):469-475.

(132) Statens Serum Institut. WHO Collaborating Centre for Reference and Research on
Escherichia and Klebsiella: Identification of three vtx1 and

seven vtx2 subtypes of Verocytotoxin encoding genes of Escherichia coli by conventional PCR amplification. (6).

(133) Holland JL, Louie L, Simor AE, Louie M. PCR detection of Escherichia coli O157:H7 directly from stools: evaluation of commercial extraction methods for purifying fecal DNA. J Clin Microbiol 2000 Nov;38(11):4108-4113.

(134) Suzuki R, Ihira M, Enomoto Y, Yano H, Maruyama F, Emi N, et al. Heat denaturation increases the sensitivity of the cytomegalovirus loop-mediated isothermal amplification method. Microbiol Immunol 2010 Aug;54(8):466-470.

(135) Kamachi K, Toyoizumi-Ajisaka H, Toda K, Soeung SC, Sarath S, Nareth Y, et al. Development and evaluation of a loop-mediated isothermal amplification method for rapid diagnosis of Bordetella pertussis infection. J Clin Microbiol 2006 May;44(5):1899-1902.

(136) Boyanton BL,Jr, Sural P, Loomis CR, Pesta C, Gonzalez-Krellwitz L, Robinson-Dunn B, et al. Loop-mediated isothermal amplification compared to real-time PCR and enzyme immunoassay for toxigenic Clostridium difficile detection. J Clin Microbiol 2012 Mar;50(3):640-645.

(137) Parida MM. Rapid and real-time detection technologies for emerging viruses of biomedical importance. J Biosci 2008 Nov;33(4):617-628.